https://dx.doi.org/10.1016/j.jcsr.2018.01.008

Numerical Investigation into High Strength Q690 Steel Columns of Welded H-sections under Combined Compression and Bending

Tian-Yu Ma[1,2], Guo-Qiang Li[1,3,*], Kwok-Fai Chung[2,4]

[1] *College of Civil Engineering, Tongji University, Shanghai, China*
[2] *Department of Civil and Environmental Engineering, the Hong Kong Polytechnic University, Hong Kong SAR, China*
[3] *State Key Laboratory for Disaster Reduction in Civil Engineering, Tongji University, Shanghai, China*
[4] *Chinese National Engineering Research Centre for Steel Construction (Hong Kong Branch), Hong Kong SAR, China*

Abstract: In conjunction with the experimental investigation described in the paper [1], a numerical modeling programme has been carried out to investigate further the structural behaviour of high strength Q690 steel columns of welded H-sections under combined compression and bending. Finite element (FE) models were developed by using the FE package ABAQUS. Geometrical and material non-linearities were incorporated in the FE models. Through the validation against the experimental results, these FE models showed excellent capability of replicating the key test results, including failure modes, failure loads and full load-axial deformation and load-lateral deflection histories. Upon validation of the FE models, parametric studies were conducted focusing on the effect of member residual stresses and material yield to tensile strength ratios. Then a large number of FE models were established to generate additional structural performance data over a wide range of cross-section dimensions, member slendernesses and initial loading eccentricity ratios. The FE model results were then compared with the design buckling resistances of columns under combined compression and bending according to the current European Standard EN 1993-1-1, American Specification ANSI/AISC 360-16 and Chinese Standard GB 50017-2003. The comparisons revealed that by properly selecting design parameters, the design rules in EN 1993-1-1 and GB 50017-2003 could provide close and safe predictions to the buckling resistances of Q690 steel columns of welded H-sections while the design rules in ANSI/AISC 360-16 was readily applicable to the design of Q690 steel columns of welded H-sections.

Keywords: **High strength steel; Welded H-sections; Combined compression and bending; Numerical simulation; Design proposal**

1 Introduction

Structural steel materials with nominal yield strengths equal to or higher than 460 N/mm^2, widely known as high strength steels, can potentially lead to slenderer and lighter structures. In the recent decades, high strength steel materials with various steel grades have been innovatively used in many heavily loaded and long spanned structures. The reduced deadweight of high strength steel structures allows for lower construction costs and transportation workloads. Compared with those conventional steel materials, high strength steel materials exhibit a reduced ductility with a smaller elongation at fracture and a limited degree of strain hardening after yielding. Moreover, the values of tensile to yield strength ratios are also decreased. Some structural design codes have covered the design of steelworks made of high strength steel materials with some restrictions due to their inferior ductility and strain-hardening characteristics. However, these recommended design rules are mainly based on test data for conventional strength steel materials and further investigation on the applicability of such design rules to high strength steel materials is required.

Recently, several researchers have investigated the structural behavior of high strength steel columns under compression. Through the tests on stocky columns of welded sections, it was preliminarily concluded that the plate slendernesses limits for yielding obtained from conventional steel sections were also applicable to similar sections made of high strength steel [2] [3] [4] [5], however, sufficient deformation capacities could not be guaranteed if the plate slenderness limits for conventional steel compact sections were simply extended to high strength steel sections [6]. Some compression tests were conducted on slender columns of welded sections with steel grades from 460 to 960 N/mm^2 [7]–[13]. Those sections with steel grades higher than 460 N/mm^2 exhibited significantly higher buckling resistances than those similar sections made of conventional steel materials on a non-dimensional basis. Those resistance improvements were mainly attributed to higher yield strengths and lower residual stress to yield strength ratios. Besides, the end restraints and limited initial out-of-straightnesses also contributed to the resistance improvements.

The investigations on structural behavior of high strength steel columns under combined compression and bending remain scarce. Kim et al. [14] tested stocky columns of welded sections with 650 N/mm^2 steel and found that the design code ANSI/AISC 360-10 [15] adopted a fairly conservative method to evaluate the sectional resistances of high strength steel welded sections. Nie et al. [16] examined the overall buckling behavior of slender columns of welded box sections with 460 N/mm^2 steel and made design recommendations based on the comparisons between numerical results and column curves in different codes. Usami et al. [17] [18] conducted eccentric compression tests on columns with slender sections made of 460 and 690 N/mm^2 and verified an effective width approach with respect to interaction between local and

overall buckling. Shen [19] proposed a modification factor to the design of 460 N/mm^2 steel welded box-sections with slender webs based on the design rules in GB 50017-2003 [20].

Currently, there are a number of design codes whose scopes of applicability cover or may be readily expanded to cover steel sections made of high strength Q690 steel materials. Based on the design rules applicable to steel grades from S235 to S460 given in EN 1993-1-1 [21], EN 1993-1-12 [22] gives supplementary rules to steel grades up to S700. ANSI/AISC 360-16 [23] covers steel grades up to 690 N/mm^2 (ASTM A514 and A709 steel) while GB 50017-2003 [20] only applies to steel grades from Q235 to Q420. As the development of these design codes was based on the studies on conventional strength steel materials, there is a concern on the applicability of those rules to high strength steel materials.

In order to promote an effective use of high strength steel sections in building construction, a comprehensive research programme was undertaken to investigate structural behavior of Q690 steel columns of welded H-sections. The experimental programme has been presented in the companion paper [1] and the parallel numerical programme is presented in this paper. In this numerical programme, validated numerical models were initially developed through accurate replication of the test results presented in paper [1]. Parametric studies were performed subsequently to examine further the influences of member residual stresses and material tensile to yield strength ratios on the structural response of high strength Q690 columns of welded H-sections under combined compression and bending. Finally, the assessment on the applicability of design rules in different design codes was conducted through the comparison with FE model results.

2 Finite element model

In the experimental programme, a total of 8 slender columns with four sections of different cross-sectional dimensions were tested successfully under eccentric loads. The nominal dimensions for those sections and their section classifications according to EN 1993-1-1 and ANSI/AISC 360-16 are shown in Figure 1.

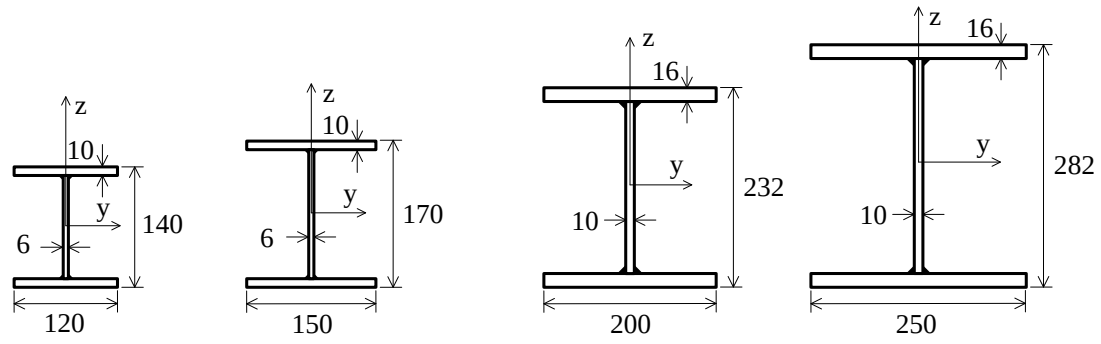

Class 1
Compact
a) Section H1

Class 3
Non-compact
b) Section H2

Class 2
Compact
c) Section H3

Class 3
Non-compact
d) Section H4

Figure 1 Norminal cross-sectional dimensions of welded H-sections

In this section, the key characteristics of the finite element models are presented. Geometrical and material non-linearities were incorporated in the FE models in order to replicate the structural behavior observed in the experimental programme. Those FE models were validated through the comparison of numerical results with the relevant test data.

2.1 Elements and basic modeling assumptions

The general purpose finite element analysis package ABAQUS (version 6.11) was employed throughout this study. Shell elements were adopted to discretize the high strength Q690 steel columsn of welded H-sections. Shell elements are frequently used in the modeling of thin-walled metallic sections and they have been successfully implemented in other studies [10] [24] [25] [26]. The finite element type S4R was selected from the ABAQUS element library and it was a four-noded, doubly curved general-purpose shell element with reduced integration and finite membrane strains. A mesh convergence study was carried out to establish a sufficiently refined mesh size which provides accurate results with practical computational times. For each flange and web, the adopted mesh size along the lateral direction of the plate was 1/20 of the plate width while the adopted mesh size along the longitudinal direction was 1/40 of the plate length. The measured geometrical and material mechanical properties obtained prior to testing were used in the finite element models. The initial out-of-straightnesses were incorporated into the models in the form of the lowest elastic overall buckling mode shape, obtained from a linear perturbation buckling analysis. The initial out-of-straightnesses were applied by using the "*IMPERFECTIONS" command with amplitudes equal to the measured values prior to testing. The modeling of residual stresses was achieved by setting the initial stresses of the shell elements. Boundary conditions were applied to model the pin-ended conditions at both ends of the columns.

For each finite element model, the simulation consisted of two analyses. The first analysis was a linear perturbation buckling analysis, which was performed on a "perfect" column. The purpose of this analysis was to obtain the lowest elastic overall buckling mode shape, which would be employed as the shape of the initial out-of-straightness of the column in subsequent analysis. The second analysis was a static analysis using the modified Riks method, which was performed on an "imperfect column" with both material and geometrical non-linearities. The purpose of this analysis was to trace the full load-deformation response of the specimens, including the post-ultimate path.

2.2 Material modelling

The measured Q690 steel stress-strain curves were utilized in the development of the finite element models. The material behaviour was modeled as an elastic-linear hardening relationship with a Von Mises yield criterion and isotropic hardening, as shown in Figure 2. It should be noted that ABAQUS requires the input of the material true stress-logarithmic plastic strain curves. True stress, σ_{true}, and logarithmic plastic strain, ε_{log}^{pl}, were obtained from the engineering stress-strain data as given by Eqs. (1) and (2) respectively, where σ_{eng} and ε_{eng} are engineering stress and engineering strain respectively and E is Young's modulus. The material true stress-logarithmic plastic strain behaviour was generated from the engineering stress-strain data obtained from standard tensile tests. The key parameters in true stress-logarithmic plastic strain behavior for all the Q690 steel plates are shown in Table 1.

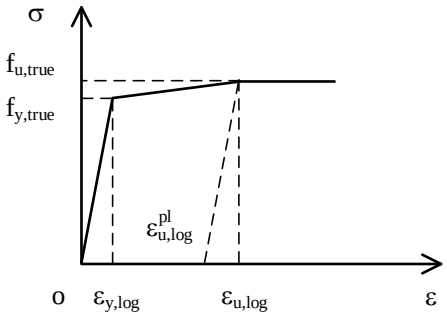

Figure 2 True tress-logarithmic strain relationships for Q690 steel plates

$$\sigma_{true} = \sigma_{eng}\left(1+\varepsilon_{eng}\right) \quad (1)$$

$$\varepsilon_{log}^{pl} = \ln\left(1+\varepsilon_{eng}\right) - \frac{\sigma_{true}}{E} \quad (2)$$

Table 1 True stress-logarithmic plastic strain relationship for Q690 steel plates in FE models

Steel plate	Nominal thickness (mm)	Young's Modulus E (kN/mm^2)	True yield strength $f_{y,true}$ (N/mm^2)	True tensile strength $f_{u,true}$ (N/mm^2)	Logarithmic plastic strain at $f_{u,true}$ $\varepsilon_{u,log}^{pl}$
T06	6	210	766	863	0.053
T10	10	212	756	849	0.064
T16	16	209	800	900	0.060

2.3 Residual Stresses

Residual stresses arise in welded steel sections due to differential cooling. These stresses can have a significant effect on the buckling behavior. A residual stress measurement was conducted by Liu and Chung [27] in parallel with the experimental programme of Q690 steel columns welded H-sections under eccentric loads. The hole-drilling method was adopted to measure the residual stresses in Sections H1 to H4. Blind holes were drilled on the outer surfaces of the flanges and on both surfaces of the webs. Locations of these holes were twice of the section height away from the column ends to avoid end effects. The flange tips were found to be in residual compression whilst the web-to-flange junction was in residual tension. A residual stress pattern was proposed for these Q690 steel columns of welded H-sections in form of piecewise linearity. The shape of the residual stress pattern is shown in Figure 3 (a) and the amplitudes are summarized in Table 2, where $f_{r,ft}$ and $f_{r,fc}$ are tensile and compressive residual stresses in flanges respectively and $f_{r,wt}$ and $f_{r,wc}$ are tensile and compressive residual stresses in webs respectively. Besides, the residual stress pattern for conventional steel columns of welded H-sections with flame-cut flange plates assumed by European Convention for Constructional Steelwork (ECCS) is shown in Figure 3 (b). It is found that the tensile residual stress ratios near the flange-to-web conjunctions of Q690 steel columns of welded H-sections are significantly smaller than the ratio assumed by ECCS. For Q690 steel columns of welded H-sections, the tensile residual stresses are far below the yield strength. As for the compressive residual stress ratios in the flange tips, the ratios of H3 and H4 were significantly smaller than the assumed value, while the ratios of H1 and H2 were close to the assumed value. This should be due to the narrow flanges in Sections H1 and H2, where large compressive residual stresses arose to balance the tensile residual stresses.

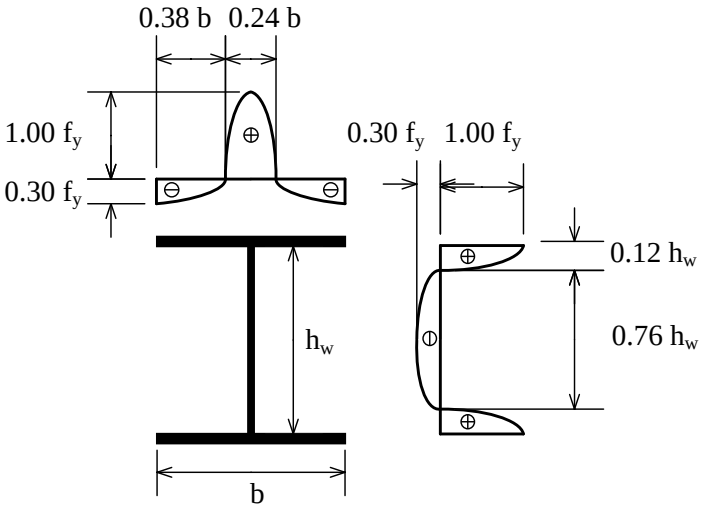

a) Q690 steel columns of welded H-sections

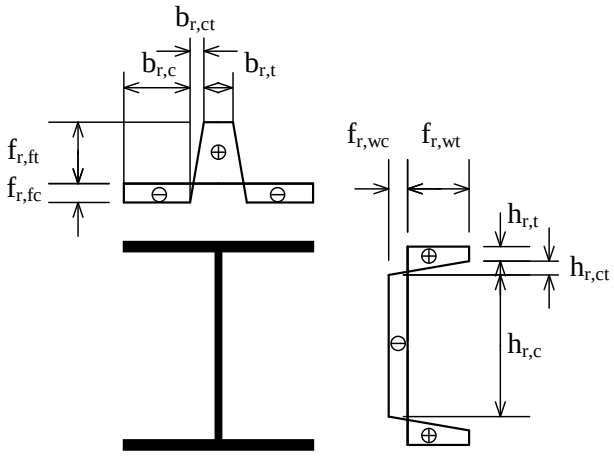

b) ECCS assumed model

Figure 3 Residual stress distribution model

Table 2 Residual stress amplitudes for Q690 steel columns of welded H-sections

Section	Residual stress				Residual stress ratio				Residual stress zone width					
	$f_{r,ft}$ (N/mm^2)	$f_{r,fc}$ (N/mm^2)	$f_{r,wt}$ (N/mm^2)	$f_{r,wc}$ (N/mm^2)	$f_{r,ft}/f_y$	$f_{r,fc}/f_y$	$f_{r,wt}/f_y$	$f_{r,wc}/f_y$	$b_{r,c}$ (mm)	$b_{r,ct}$ (mm)	$b_{r,t}$ (mm)	$h_{r,c}$ (mm)	$b_{r,ct}$ (mm)	$b_{r,t}$ (mm)
H1	+357	-211	+357	-66	+0.47	-0.28	+0.47	-0.09	23	30	14	94	7	6
H2	+451	-204	+451	-59	+0.60	-0.27	+0.59	-0.08	36	32	14	128	5	6
H3	+368	-147	+368	-148	+0.46	-0.18	+0.49	-0.20	50	43	14	106	37	10
H4	+462	-137	+462	-177	+0.58	-0.17	+0.61	-0.23	75	42	16	132	49	10
ECCS assumed model	---	---	---	---	+1.00	-0.30	---	---	---	---	---	---	---	---

Residual stresses were introduced into the finite element models by setting the initial stresses in the partitions of web and flanges. Each web and flange plate was equally divided into 20 partitions and the initial stress in each partition was equal to the mid-point of the linear variation in stress over the partition length. The stresses were applied using the "*INITIAL CONDITIONS" command.

2.4 Boundary conditions and interfaces

The boundary conditions were carefully selected to simulate the experimental setup. In the experiments, a pair of attachments were connected to the columns through bolts. These attachments enabled free rotations of the columns about minor axes of their cross-sections and they also provided initial loading eccentricities. Therefore, in the numerical model, the experimental setup was represented by endplates and reference points at both ends of the column, as shown in Figure 4. The top and bottom end sections of each column were "tied" to the inner surfaces of the nearby endplates respectively. The nodes of each endplate were "coupled" to an eccentric reference point, allowing rotation about the minor axis at one end and the same rotation plus longitudinal translation at the loaded end, in order to simulate the boundary conditions. The distance between the eccentric reference points and the corresponding end sections along the x axis were equal to the height of the attachment plus the thickness of the welded endplate (30 mm) in order to accurately model the effective length, L_{eff}. In addition, the top and bottom eccentric reference points were offset laterally from the longitudinal axis of H-sections by a distance equal to the calculated initial loading eccentricities e_A and e_C along y axis respectively. The initial loading eccentricities were calculated by using the strain gauge readings and lateral deflections at relevant sections during the tests.

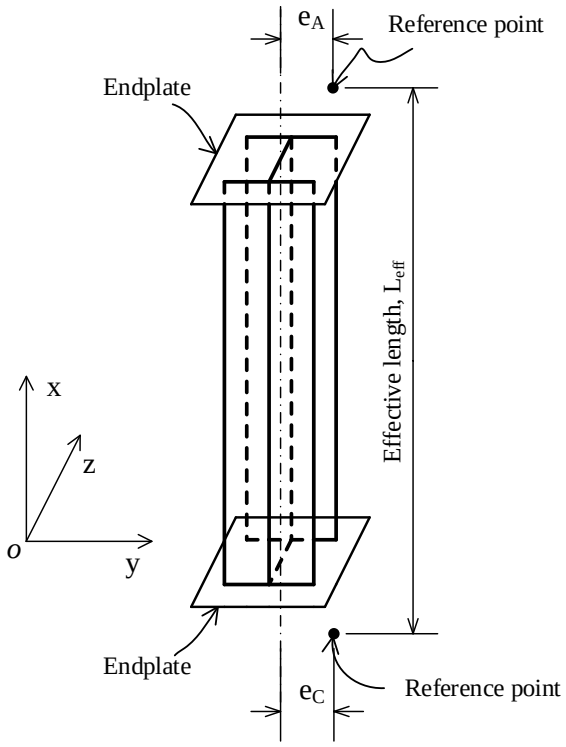

Figure 4 Boundary conditions and interfaces in FE model

2.5 Validation of finite element models

Validation of finite element models was based on the comparison of obtained numerical results with relevant test data. The same as the test results, all the FE models failed in overall flexural buckling about minor axes of their cross-sections. The typical failure modes observed in the test and the FE model are presented in Figure 5. The buckling resistances of FE models, N_{FEM}, and the buckling resistances of test specimens, N_{test}, are compared in Table 3. It is found that the resistance ratios, N_{test}/N_{FEM}, range from 94.2% to 106.0% with an average of 1.01. Thus, the FE models are able to capture the observed failure modes and buckling resistances. In addition, the applied load N versus lateral deflection Δy curves from the FE models and the tests are shown in Figure 6 and the applied load N versus axial deformation Δx curves from the FE models and the corresponding curves from the tests are shown in Figure 7. It is demonstrated that the curves from FE models coincide well with the corresponding curves from tests. Overall, it is concluded that the finite element models are capable of replicating the key test results.

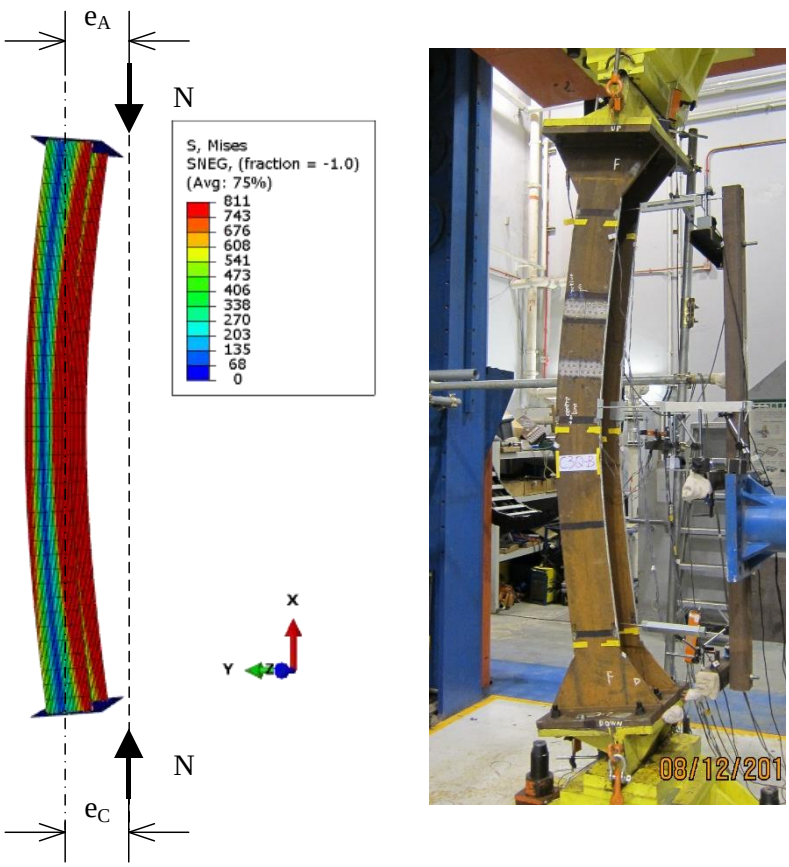

a) FE model b) Test

Figure 5 Typical failure modes observed in the FE models and tests

Table 3 Buckling resistances from FE models and tests

Test	Buckling resistance		$\frac{N_{test}}{N_{FEM}}$
	N_{FEM} (kN)	N_{test} (kN)	
EH1P	309	328	1.06
EH2P	500	527	1.05
EH3P	1,703	1,698	1.00
EH4P	2,675	2,660	0.99
EH1Q	256	250	0.98
EH2Q	418	418	1.00
EH3Q	1,356	1,376	1.01
EH4Q	2,274	2,276	1.00
Average	---	---	1.01

Notes: 1. The first character "E" stands for "Eccentrically loaded column";
2. The second and the third characters indicate the sectional designation;
3. The last character indicates the effective length of the specimen.

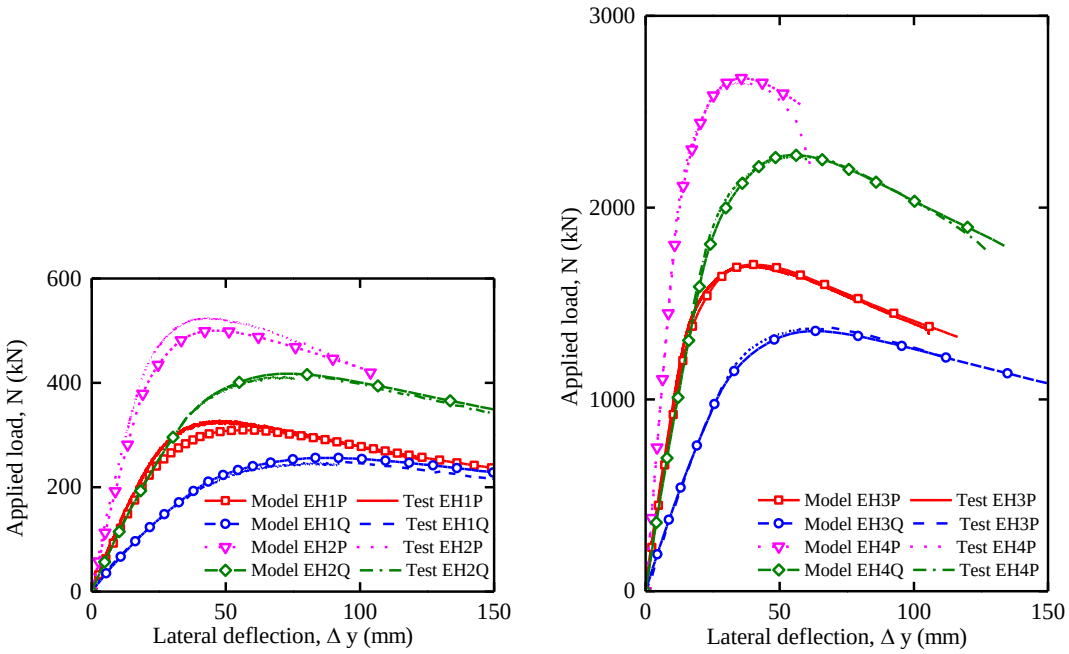

a) Sections H1 and H2 b) Sections H3 and H4

239 **Figure 6 Comparison on load versus lateral deflection curves between tests and**
240 **FE models**

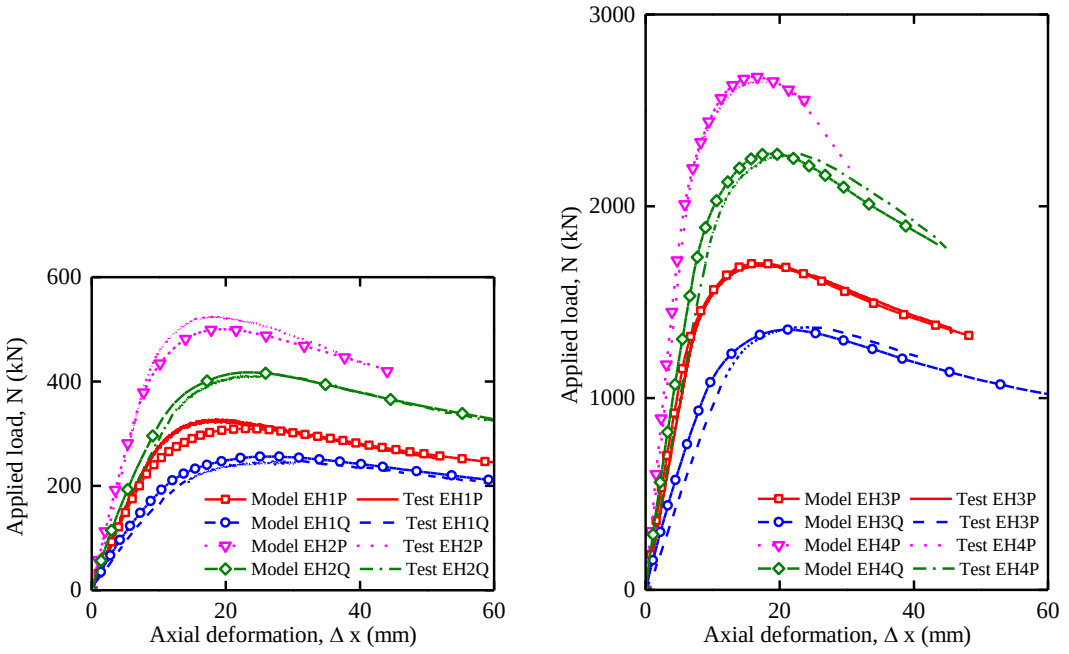

a) Sections H1 and H2 b) Sections H3 and H4

241 **Figure 7 Comparison on load versus axial deformation curves between tests and**
242 **FE models**

243

3 Parametric studies

Having validated the numerical models against the experimental results, a series of parametric studies were performed, focusing on residual stresses and material tensile to yield strength ratios. The measured residual stress ratios of Q690 steel columns of welded H-sections were found to be significantly smaller than the assumed values by ECCS for conventional steel columns of welded H-sections, thus the adverse effect from residual stresses on Q690 steel columns of welded H-sections were anticipated to be less than that on conventional steel columns of welded H-sections. The degree of residual stress effect for Q690 steel and Q235 steel columns of welded H-sections will be compared in the following studies. Another factor that may affect the buckling resistances of Q690 welded H-sections is material tensile to yield strength ratios. The tensile to yield strength ratios indicate the abilities of strain hardening of the materials. For conventional steel material, strain hardening develops at the end of a long yield plateau. In the simulation of conventional steel members whose resistance is dominated by instability, an elastic-perfectly plastic model is practically adopted and the strain hardening is neglected. However, for Q690 steel, the strain hardening starts once the material is yielding. Therefore, for Q690 steel columns of welded H-sections, the neglection of strain hardening may lead to a conservative design. The contribution of strain hardening to the buckling resistances is related with the tensile to yield strength ratios. In the following studies, the effect of tensile to yield strength ratios are evaluated for Q690 steel columns of welded H-sections under combined compression and bending.

In the generation of FE models, all the steel columns were modeled by using shell elements S4R. Section H3 was selected as a typical cross-section size. The non-dimensional slendernesses of these FE models ranged from 0.6 to 1.8 with an interval of 0.4. To normalize the initial loading eccentricity with the cross-sectional properties, an initial loading eccentricity ratio is defined by Eq. (3), where e is initial loading eccentricity, A is area of cross-section and W_{el} is elastic modulus of cross-section. For each non-dimensional slenderness, the initial loading eccentricity ratios varied from 0.0 (compression only) to 20.0 (combined compression and bending).

$$\varepsilon = \frac{eA}{W_{el}} \tag{3}$$

The shape of the initial out-of-straightness was assumed to be a sinusoidal shape and the amplitude was replaced by $L_{eff}/1000$. The initial out-of-straightness and the initial loading eccentricity were positioned on different sides of the longitudinal axis of the welded H-sections.

3.1 Residual stresses

To evaluate the effect of residual stresses on Q690 steel columns of welded H-sections, buckling resistances were obtained from two groups of FE models, in which one with residual stresses and the other one without residual stresses. The residual stress amplitudes for Q690 steel welded H-section H3 were shown in Table 2.

A total of 240 numerical models were established and their information is summarized in Table 4. In this study, the overall flexural buckling was not restricted in minor axis but extended to major axis. The material behaviour of Q690 steel was modeled as an elastic-linear hardening relationship, as shown in Figure 2. The mechanical properties of Q690 steel were obtained in standard the tensile tests and the key parameters in true stress-logarithmic plastic strain behavior are shown in Table 1.

Table 4 FE model information for the evaluation of effect of residual stresses

Group	Bending axis	Steel grade	Residual stresses	Initial out-of-straightness v	Model numbers	Non-dimensional Slenderness
1	Major	690	No	$L_{eff}/1000$	60	0.6 / 1.0 1.4 / 1.8
2			Yes		60	
3		235	No		60	
4			Yes		60	
5	Minor	690	No		60	
6			Yes		60	
7		235	No		60	
8			Yes		60	

To compare the effect of residual stresses on Q690 steel columns of welded H-sections with that on Q235 steel columns, FE models with Q235 steel were generated and their model information is also summarized in Table 4. The residual stress pattern for Q235 steel columns of welded H-sections is shown in Figure 3 (b). The material behaviour of Q235 steel was modeled as a multi-linear relationship, as shown in Figure 8. The yield strength was taken to be its nominal value, 235 MPa and the tensile strength was 370 MPa according to GB/T 700 [28] and EN 10025-2 [29]. The strain at yield plateau end, $\varepsilon_{st,log}$, and the ultimate strain, $\varepsilon_{u,log}$ were based on the suggestions given by Shi et al [30]. The key parameters in true stress-logarithmic plastic strain behavior are shown in Table 5.

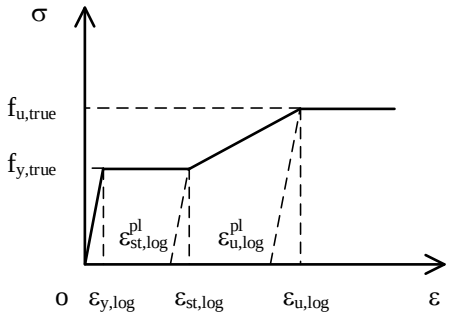

Figure 8 True tress-logarithmic strain relationships for Q235 steel plates

Table 5 True stress-logarithmic plastic strain relationship for Q235 steel plates in FE models

Young's Modulus E (kN/mm^2)	True yield strength $f_{y,true}$ (N/mm^2)	True strength onset of strain hardening $f_{st,true}$ (N/mm^2)	logarithmic plastic strain onset of strain hardening $\varepsilon^{pl}_{st,log}$	True tensile strength $f_{u,true}$ (N/mm^2)	logarithmic plastic ultimate strain $\varepsilon^{pl}_{u,log}$
210	235	240	0.024	444	0.182

Figure 9 and Figure 10 depict the normalized compression and bending relationships of FE models, arranged by non-dimensional slenderness, $\bar{\lambda}$. In these figures, N_{FEM} is the buckling resistance obtained from the finite element models, $M_{FEM} = N_{FEM} \cdot e$, $N_{pl} = A \cdot f_y$ and M_{pl} is the sectional plastic resistance to bending moment. It is found that:

1) The presence of residual stresses reduces the buckling resistances of both Q690 and Q235 steel columns of welded H-sections under combined compression and bending. Compared with Q235 steel columns of welded H-sections, the effect degree becomes less on Q690 steel columns of welded H-sections with the same non-dimensional slenderness and initial loading eccentricity ratio.

2) For both Q690 and Q235 steel columns of welded H-sections, when the non-dimensional slendernesses of the columns are 0.6 and 1.0, the effect of residual stresses decreases with the increase of initial loading eccentricity ratio. However, when the non-dimensional slendernesses of the columns are 1.4 and 1.8, the effect of residual stresses initially increases and subsequently decreases with the increase of initial loading eccentricity ratio.

Overall, residual stresses can significantly reduce the buckling resistances of Q690 steel columns of welded H-sections under combined compression and bending. But compared with Q235 steel columns of welded H-sections, the effect of residual stresses is decreased for Q690 steel columns of welded H-sections due to the smaller ratios of residual stresses to yield strength.

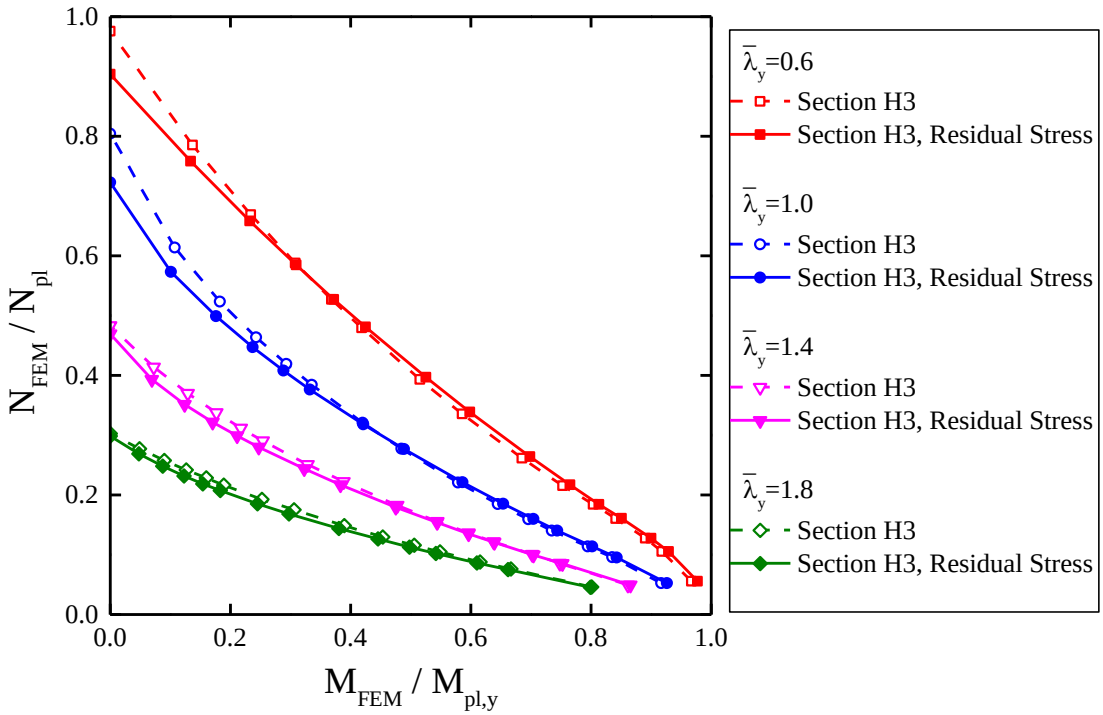

a) Q690 steel columns of welded H-sections

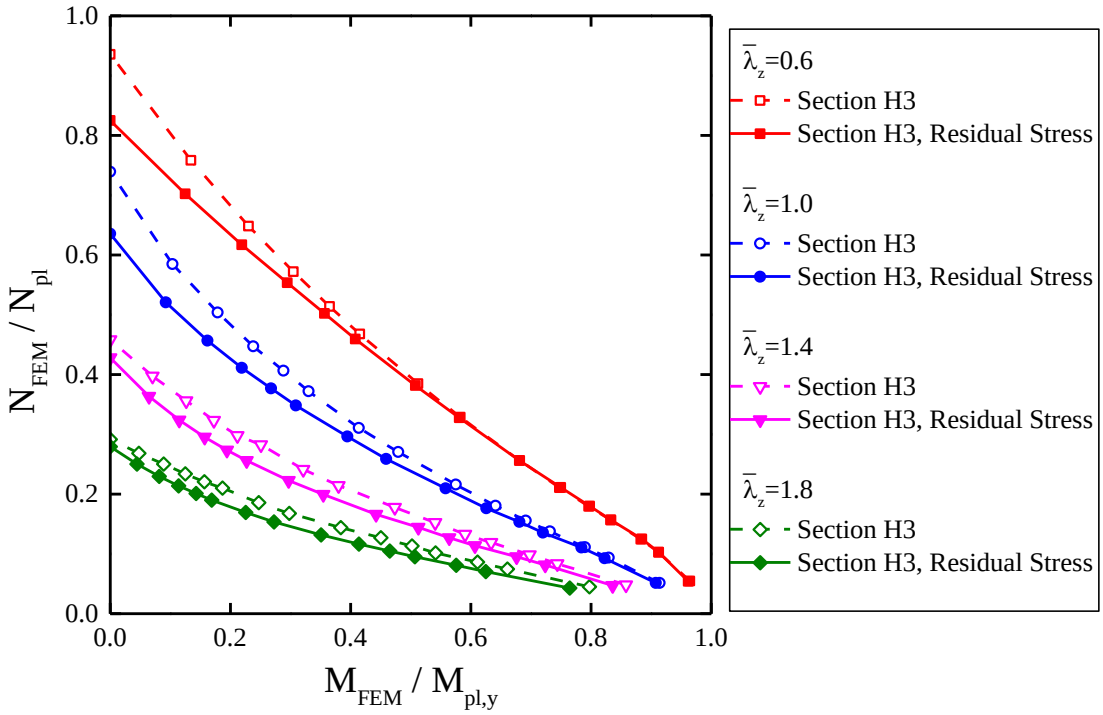

b) Q235 steel columns of welded H-sections

Figure 9 Effect of residual stresses on buckling resistances of Q690 and Q235 steel columns of welded H-sections under combined compression and major axis bending

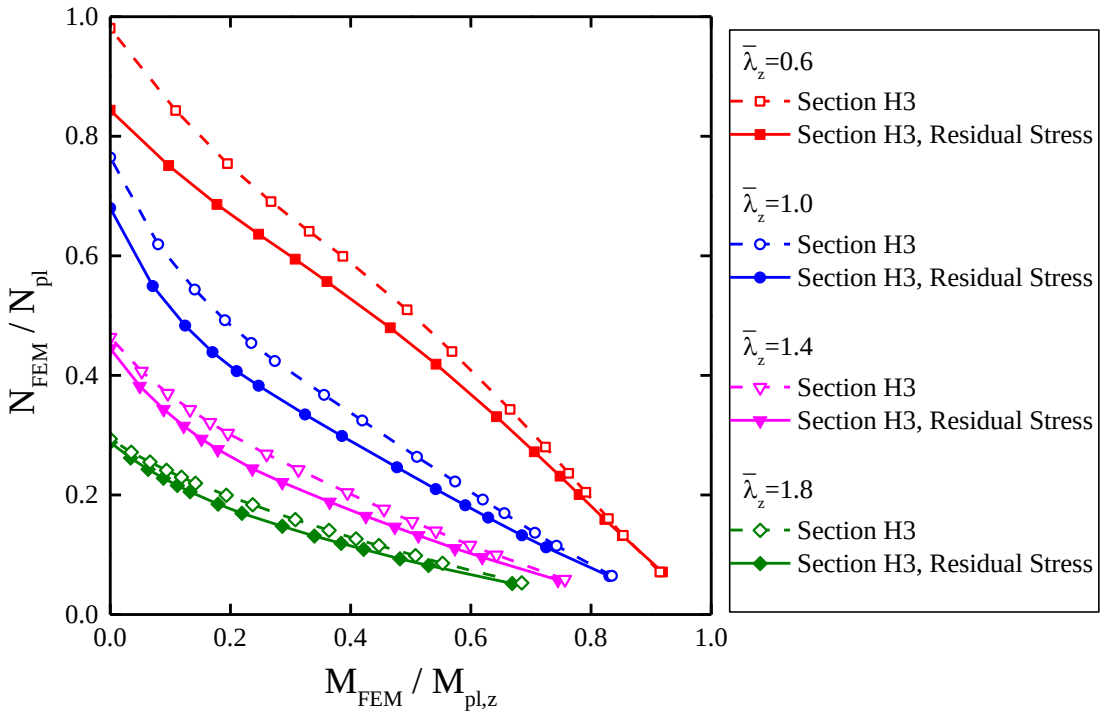

a) Q690 steel columns of welded H-sections

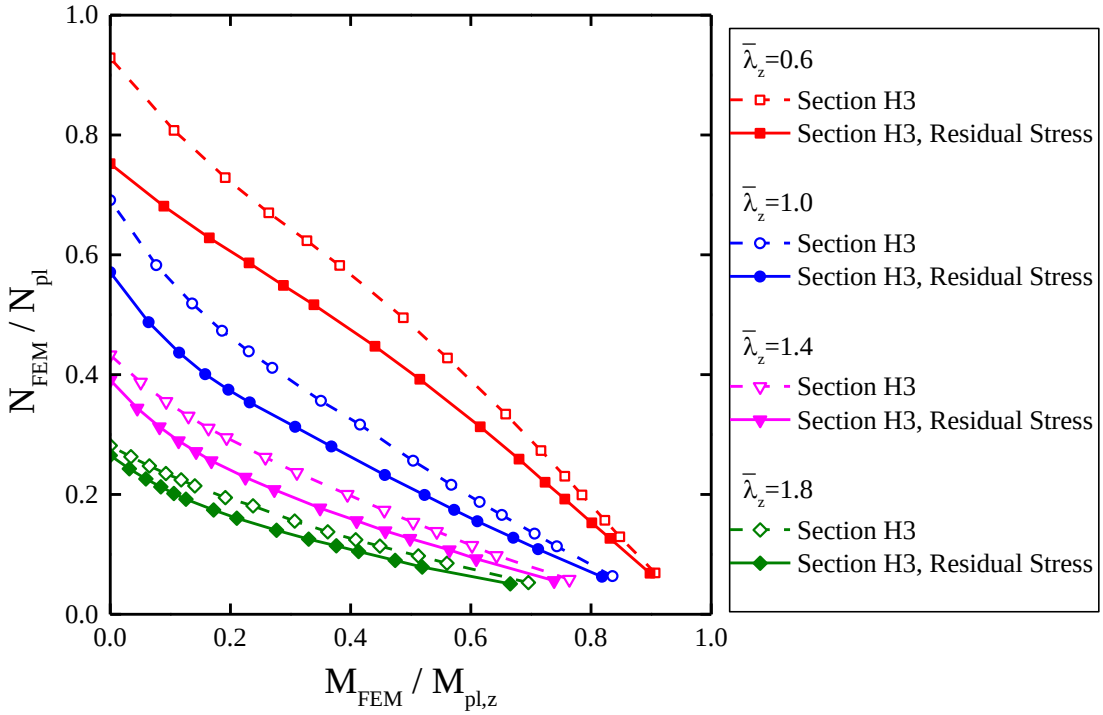

b) Q235 steel columns of welded H-sections

Figure 10 Effect of residual stresses on buckling resistances of Q690 and Q235 steel columns of welded H-sections under combined compression and minor axis bending

3.2 Tensile to yield strength ratios

To evaluate the effect of tensile to yield strength ratios on Q690 steel columns of welded H-sections, buckling resistances were obtained from FE models with two different material stress-strain models, namely, i) an elastic-linear hardening model (see Figure 2) and ii) an elastic-ideally plastic model, as shown in Figure 11. The mechanical properties of these two models are listed in Table 1 and only E and $f_{y,true}$ were included in the elastic-ideally plastic model. A total of 240 numerical models were established and their information is summarized in Table 6. The residual stress pattern for Q690 steel welded H-section H3 is listed in Table 2. The overall flexural buckling was not restricted in minor axis but extended to major axis.

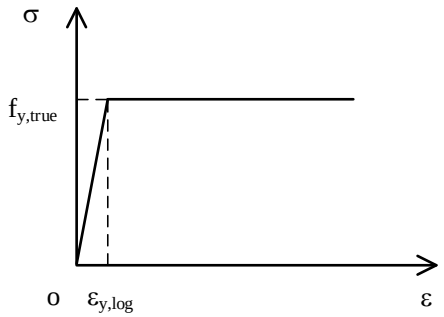

Figure 11 Elastic-ideally plastic model

Table 6 FE model information for the evaluation of effect of tensile to yield strength ratios

Group	Bending axis	Steel grade	f_u/f_y	Residual stresses	Initial out-of-straightness v	Model numbers	Non-dimensional slenderness
1	Major	690	1.00	Yes	$L_{eff}/1000$	60	0.6 / 1.0 1.4 / 1.8
2			1.05			60	
3		235	1.00			60	
4			1.57			60	
5	Minor	690	1.00			60	
6			1.05			60	
7		235	1.00			60	
8			1.57			60	

To compare the effect of tensile to yield strength ratios on Q690 steel columns of welded H-sections with that on Q235 steel columns of welded H-sections, FE models

with Q235 steel were generated and their model information is also summarized in Table 6. Two different material stress-strain models were considered, namely, i) a multi-linear model (see Figure 8), and ii) an elastic-ideally plastic model (see Figure 11). The mechanical properties of these two models are listed in Table 5 and only E and $f_{y,true}$ were excluded in the elastic-ideally plastic model. A total of 240 numerical models were established and their information is summarized in Table 6. The residual stress pattern for Q235 steel columns of welded H-sections is shown in Figure 3 (b). The overall flexural buckling was not restricted in minor axis but extended to major axis.

Figure 12 and Figure 13 depict the normalized compression and bending relationships of FE models, arranged by non-dimensional slenderness, $\bar{\lambda}$. It is found that:

1) For Q235 steel columns of welded H-sections, even though the strain hardening is considered in the stress-strain model, there is no increase in the buckling resistances of the models. This has been commonplace and lies in the fact that there is a long yield plateau in the stress-strain relationship of Q235 steel, and when the H-sections fail, significant strain hardening does not take place.

2) For Q690 steel columns of welded H-sections, when considering strain hardening, some increase in the buckling resistances of the models are visible only in columns with non-dimensional slenderness of 0.6. Because when a relatively short column fails, the strain is able to develop well beyond the yield strain, and thus the buckling resistance can take advantage of strain hardening. While when a long column fails, the strain is not able to develop beyond the yield strain and the strain hardening cannot be mobilized.

3) The maximum increase in buckling resistance improved by strain hardening is only 2.0%, thus, the elastic-ideally plastic model can be used in the modeling of buckling resistances of Q690 steel columns of welded H-sections under combined compression and bending without causing too much conservatism.

Overall, strain hardening can slightly improve the buckling resistances of Q690 steel short columns of welded H-sections, and the neglection of strain hardening will not result in a conservative design.

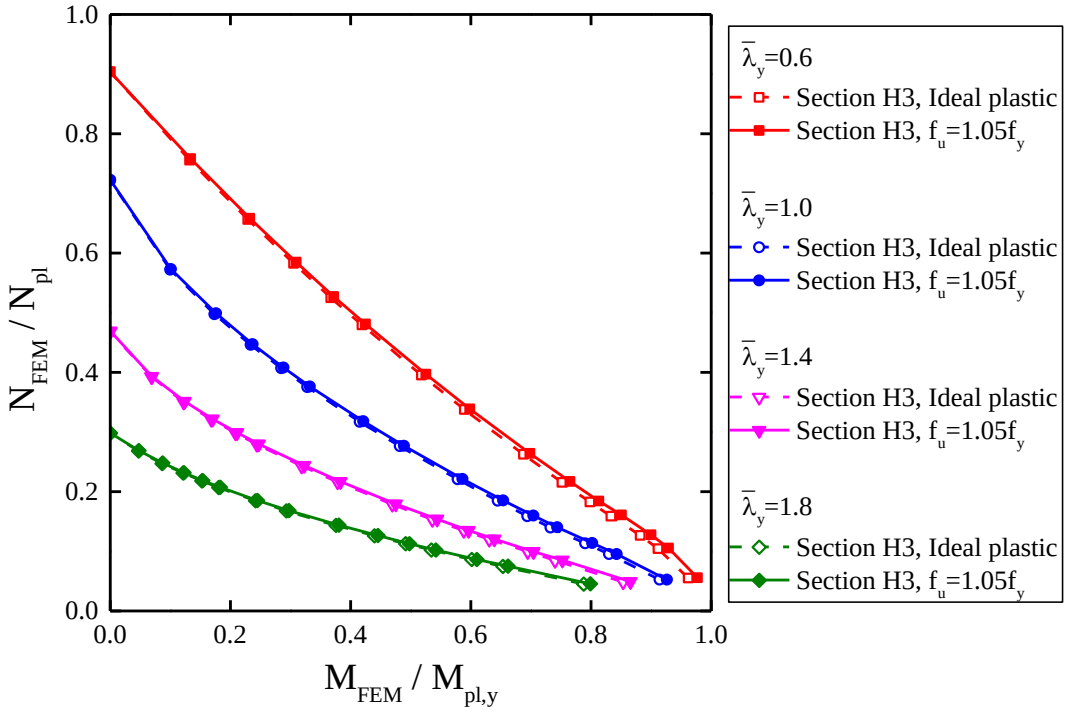

a) Q690 steel columns of welded H-sections

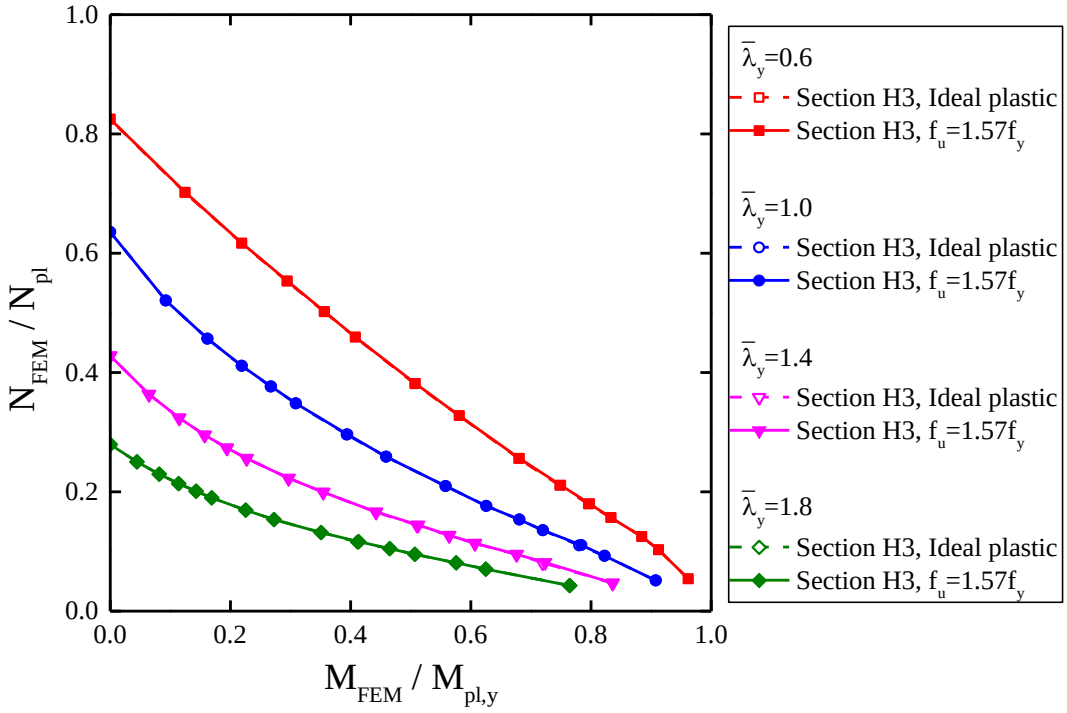

b) Q235 steel columns of welded H-sections

Figure 12 Effect of tensile to yield strength ratios on buckling resistances of Q690 and Q235 steel columns of welded H-sections under combined compression and major axis bending

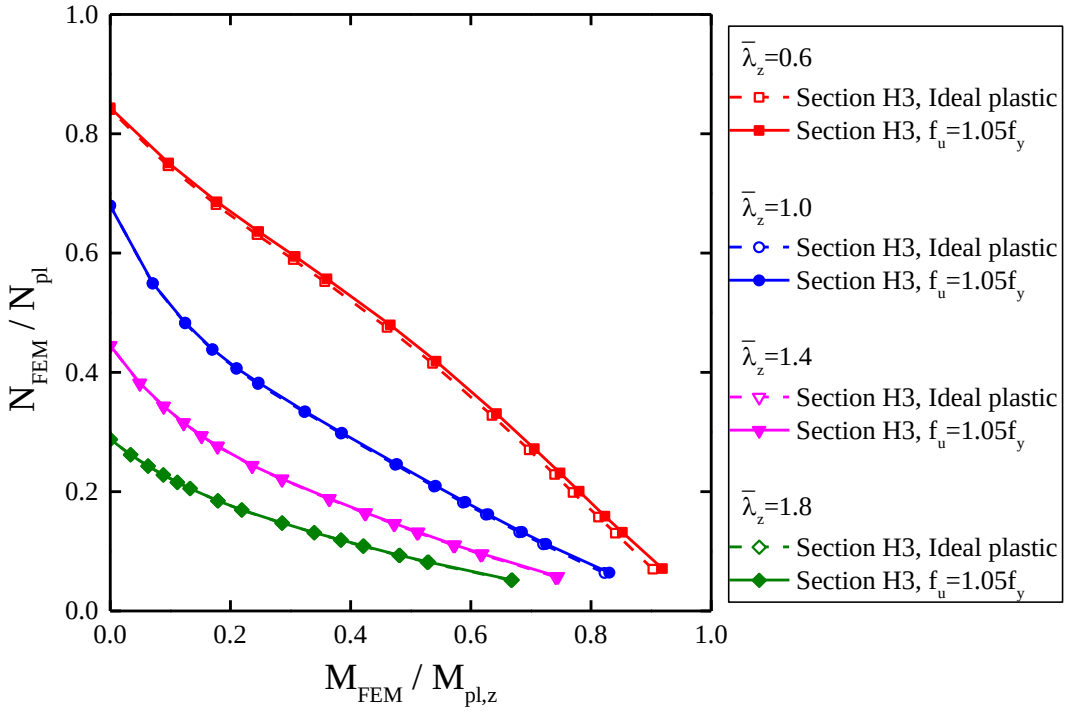

394

395 a) Q690 steel columns of welded H-sections

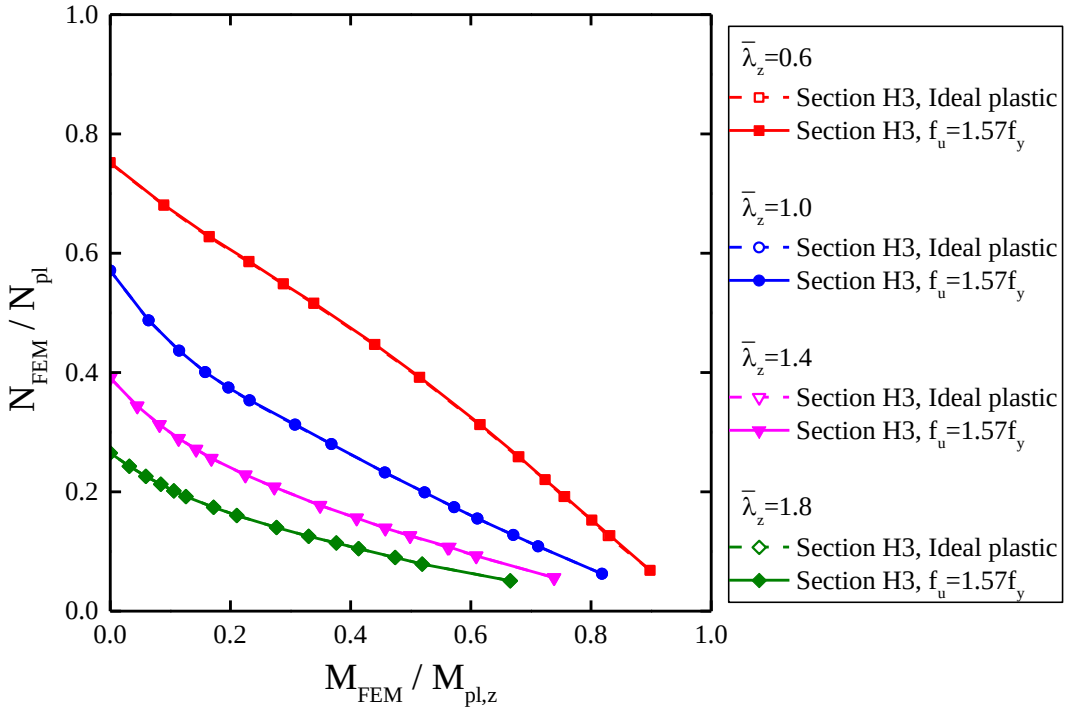

396

397 b) Q235 steel columns of welded H-sections

398 **Figure 13 Effect of tensile to yield strength ratios on buckling resistances of Q690**
399 **and Q235 steel columns of welded H-sections under combined compression and**
400 **minor axis bending**

From the parametric studies above, it is concluded that the residual stresses can significantly affect the buckling resistances of Q690 steel columns of welded H-sections under combined compression and bending. Compared with the conventional steel materials, the effect of residual stresses becomes less pronounced in Q690 steel columns of welded H-sections. It should be noted that strain hardening barely contributes to the buckling resistances of the Q690 steel columns of welded H-sections.

4 Applicability of design rules

In this section, the applicability of design rules given in EN 1993-1-1, ANSI/AISC 360-16 and GB 50017-2003 for Q690 steel columns of welded H-sections under combined compression and bending is assessed by means of the ratios of the FE to design buckling resistances. In these design rules, effects of axial compression and bending moments are summed up linearly while non-linear effects of applied bending moments are accounted for by interaction factors. Since torsional deformation is beyond the scope of this research, factors related to torsional deformation were taken to be 1.0 in the calculation of design buckling resistances.

Large numbers of FE models for Q690 steel columns of welded H-sections under combined compression and uni-axial bending were established with variations in cross-section sizes, non-dimensional slendernesses and initial loading eccentricity ratios. Cross-section sizes included Sections H1, H2, H3 and H4 and non-dimensional slendernesses included 0.6, 1.0, 1.4 and 1.8. Initial loading eccentricity ratios varied from 0.0 to 20.0. A total of 15 initial loading eccentricities were adopted, which were 0.0 to 1.0 with an interval of 0.2 and 1.5, 2.0, 3.0, 4.0, 5.0, 6.0, 8.0, 10.0 and 20.0. Residual stresses were incorporated in FE models. Initial out-of-straightnesses were taken to be sinusoidal shapes. The amplitudes of initial out-of-straightnesses complied with the theoretical background of corresponding design rules. In the assessment of both EN 1993-1-1 and GB 50017-2003, the amplitudes were 1/1000 of effective lengths while for ANSI/AISC 360-16, the amplitudes were 1/1500 of effective lengths[31].

4.1 EN 1993-1-1

According to EN 1993-1-1, the buckling resistance for a steel member under combined compression and bending should satisfy Eqs. (4) and (5).

$$\frac{N_{Ed}}{\frac{\chi_y N_{Rk}}{\gamma_{M1}}} + k_{yy}\frac{M_{y,Ed}+\Delta M_{y,Ed}}{\chi_{LT}\frac{M_{y,Rk}}{\gamma_{M1}}} + k_{yz}\frac{M_{z,Ed}+\Delta M_{z,Ed}}{\frac{M_{z,Rk}}{\gamma_{M1}}} \le 1 \qquad (4)$$

$$\frac{N_{Ed}}{\frac{\chi_z N_{Rk}}{\gamma_{M1}}} + k_{zy}\frac{M_{y,Ed}+\Delta M_{y,Ed}}{\chi_{LT}\frac{M_{y,Rk}}{\gamma_{M1}}} + k_{zz}\frac{M_{z,Ed}+\Delta M_{z,Ed}}{\frac{M_{z,Rk}}{\gamma_{M1}}} \le 1 \qquad (5)$$

where N_{Ed}, $M_{y,Ed}$, $M_{z,Ed}$ are the design values of the compression force and the moments about the major (y) and the minor (z) axes along the member, respectively;

N_{Rk}, $M_{y,Rk}$, $M_{z,Rk}$ are the characteristic values of resistances to compression force and the bending moments about the major (y) and the minor (z) axes, respectively;

$\Delta M_{y,Ed}$, $\Delta M_{z,Ed}$ are the moments due to the shift of the centroidal axes for class 4 sections;

χ_y, χ_z are the reduction factors due to flexural buckling about the major (y) and the minor (z) axes, respectively;

χ_{LT} is the reduction factor due to lateral-torsional buckling;

k_{yy}, k_{yz}, k_{zy}, k_{zz} are the interaction factors; and

γ_{M1} is the partial factor for resistance of members to instability assessed by member checks.

In the first terms of Eqs. (4) and (5), the reduction factors, χ_y and χ_z, are related to the in-plane buckling behavior, and they are determined from the studies on columns under axial compression. In EN 1993-1-1, for welded H-sections made of 690 N/mm^2 steel, curves b and c are currently proposed to calculate column buckling resistances about major (y) axis and minor (z) axis respectively. Based on the residual stress measurement and the test results in the companion paper, higher column curves may be applicable for designing Q690 steel columns of welded H-sections and the assessment of higher column curves will be conducted later. In the second terms, the reduction factor χ_{LT} is related to the lateral-torsional buckling behavior, and it was taken to be 1.0 in calculations of design buckling resistances.

The interaction factors k_{yy}, k_{yz}, k_{zy}, and k_{zz} in the second and the third terms can be obtained from two different approaches given in Annexes A and B respectively. It should be noted that the main difference between these two approaches is the way of presenting different structural effects. Annex A emphasizes transparency and each structural effect is accounted for by an individual factor. However, Annex B works with simplicity and allows some structural effects to be combined into a global factor. In this study, the design rules given in Annexes A and B in EN 1993-1-1 for Q690 steel columns of welded H-sections are assessed. It should be noted that in Annex A, the factor C_{mLT} and a_{LT} are also related to torsional deformation, and they were both taken to be 1.0. In Annex B, there are two sets of formulae for the calculation of interaction factors k_{ij}, one for members not susceptible to torsional deformations and the other one

for members susceptible to torsional deformations. The former was adopted since the effect of torsional deformation was neglected.

Figure 14 depicts the normalized compression and major axis bending relationships of FE models together with design results using curves a and b respectively. For each curve, design results following Annex A and B are compared. It can be seen that the design results using Annex B agree well with those using Annex A and Annex B is slightly more conservative than Annex A. The average ratios of FE to design buckling resistances by using curve a and curve b are summarized in Table 7. It is found that the average ratios using either curve a or curve b are slightly larger than 1.00 with standard variations smaller than 0.04. It means that both curves a and b could provide conservative predictions to buckling resistances about major axis. However, compared with curve b, the ratios using curve a are closer to 1.00. Thus, the design rules using curve a should be recommended owing to its advantage in safety and accuracy in estimating Q690 steel columns of welded H-sections under combined compression and major axis bending.

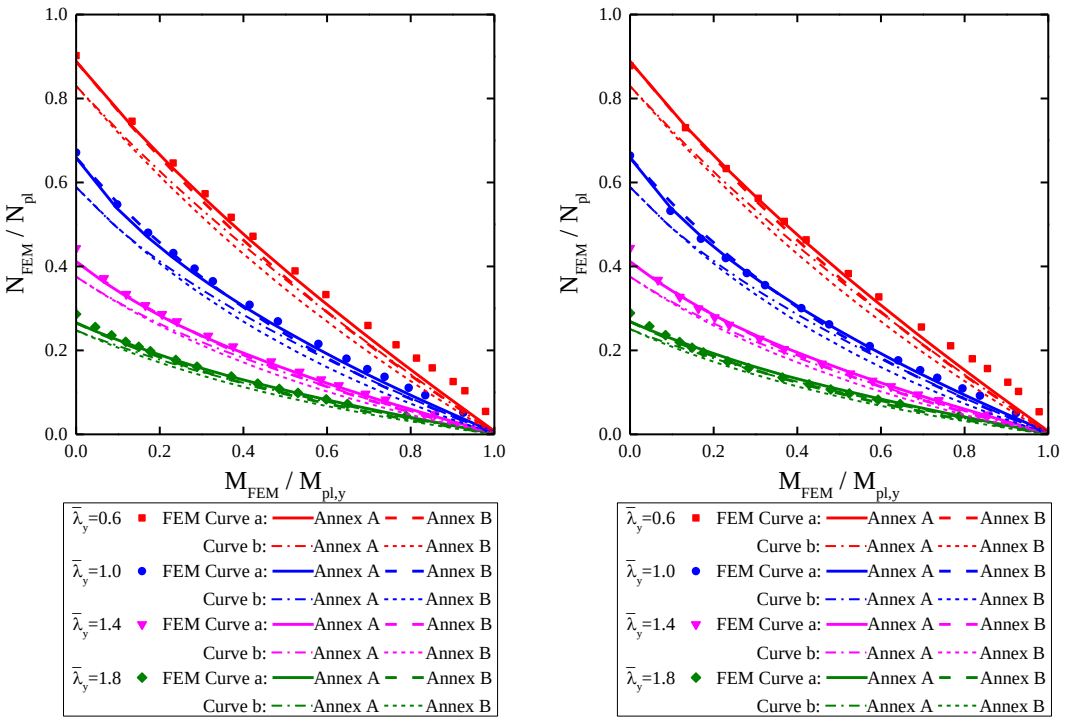

a) Section H1

b) Section H2

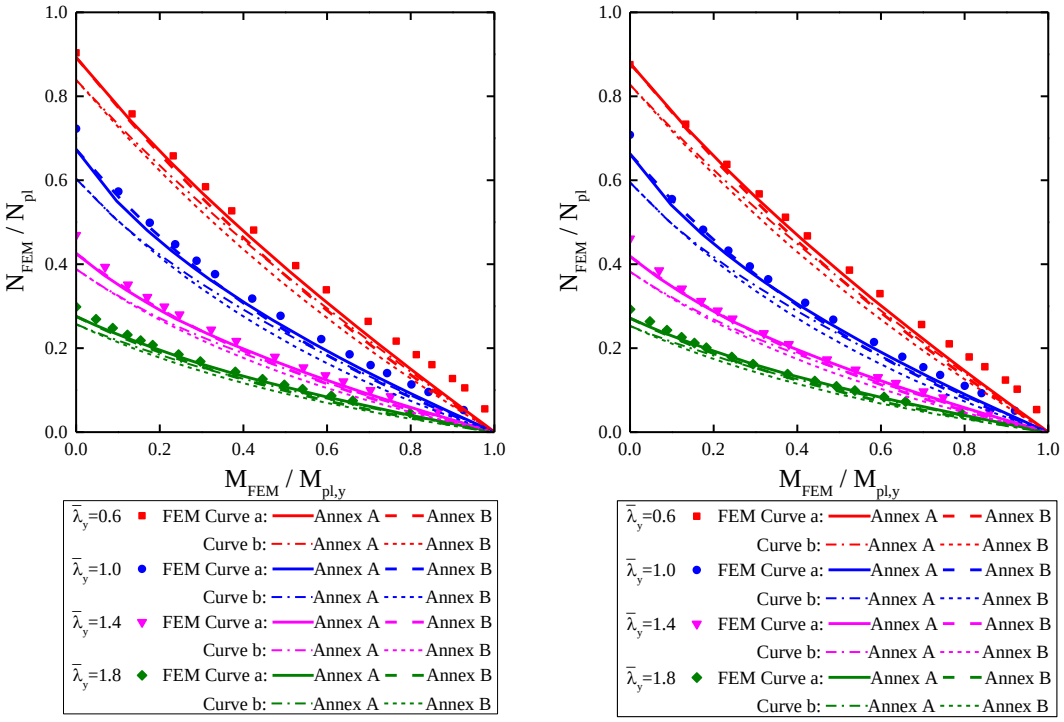

c) Section H3 d) Section H4

Figure 14 Normalized compression and major axes bending relationships of FE models and design results according to EN 1993-1-1

Table 7 Ratios of FE to design buckling resistances about major axes according to EN 1993-1-1

Section	Curve a				Curve b			
	Annex A		Annex B		Annex A		Annex B	
	Average	Standard deviation	Average	Standard deviation	Average	Standard deviation	Average	Standard deviation
H1	1.02	0.02	1.04	0.02	1.06	0.03	1.09	0.02
H2	1.01	0.03	1.02	0.03	1.05	0.03	1.07	0.02
H3	1.04	0.02	1.05	0.02	1.07	0.03	1.10	0.02
H4	1.03	0.02	1.04	0.02	1.06	0.04	1.09	0.03

Figure 15 depicts the normalized compression and minor axis bending relationships of FE models together with design results using curves b and c respectively. Large differences are found between the design results by using Annexes A and B and Annex B is fairly more conservative than Annex A. The average ratios of FE to design buckling resistances by using curve a and curve b are summarized in Table 8. For Annex A, even

494 though the average ratios using curve b are larger than 1.00, a few un-conservative
495 design results are observed in columns with non-dimensional slendernesses of 0.6 and
496 1.0. The minimum value of all the ratios using curve b is 0.96. To the contrary, only a
497 few un-conservative design results are found when using curve c and the minimum
498 value of all the ratios using curve c is 0.99. For Annex B, a few un-conservative design
499 results are found when using either curve b or c. Overall, the design rules using curve
500 c should be proposed due to acceptable accuracy in designing Q690 steel columns of
501 welded H-sections under combined compression and minor axis bending.

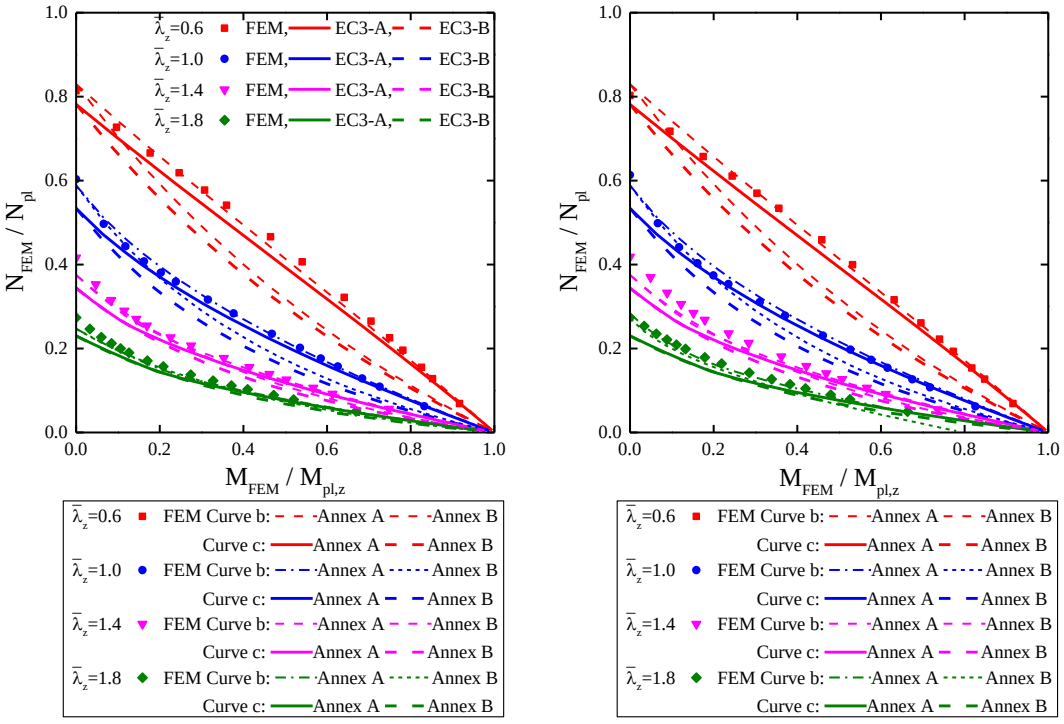

a) Section H1 b) Section H2

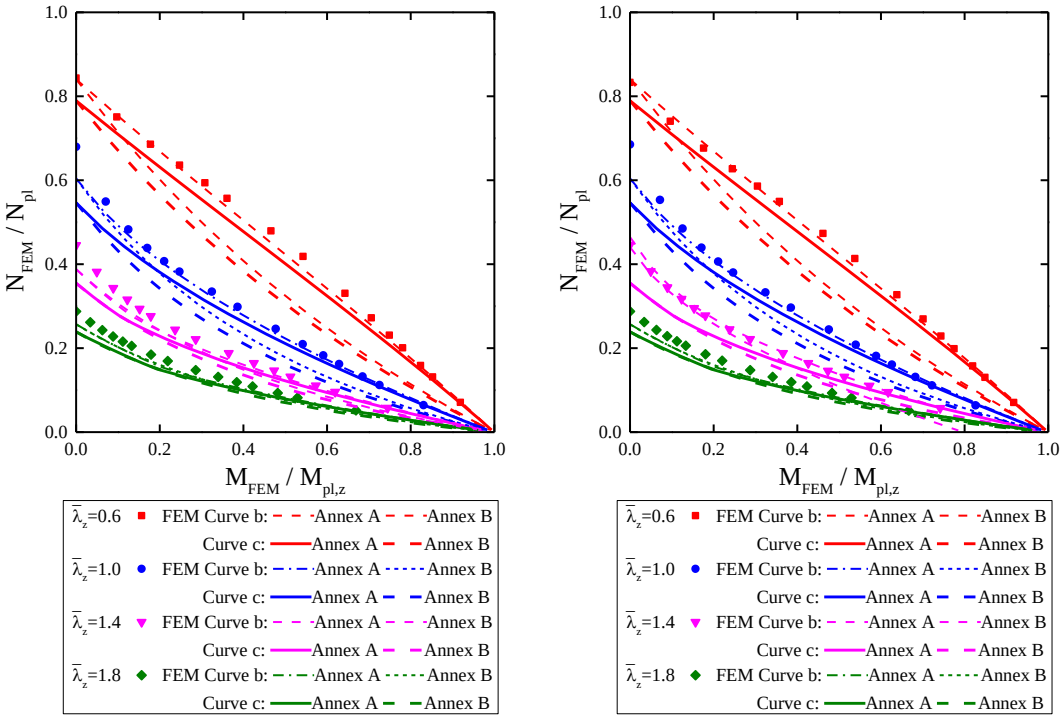

c) Section H3

d) Section H4

Figure 15 Normalized compression and minor axes bending relationships of FE models and design results according to EN 1993-1-1

Table 8 Ratios of FE to design buckling resistances about minor axes according to EN 1993-1-1

H-section	Design with curve b				Design with c urve c			
	Annex A		Annex B		Annex A		Annex B	
	Average	Standard deviation	Average	Standard deviation	Average	Standard deviation	Average	Standard deviation
H1	1.02	0.03	1.06	0.04	1.05	0.04	1.11	0.04
H2	1.02	0.05	1.07	0.04	1.06	0.06	1.12	0.04
H3	1.04	0.04	1.09	0.03	1.08	0.06	1.14	0.04
H4	1.04	0.04	1.09	0.03	1.08	0.06	1.14	0.04

4.2 ANSI/AISC 360-16

According to ANSI/AISC 360-16, the buckling resistance for a steel member under combined compression and bending should satisfy Eqs. (6) and (7).

$$\text{When } \frac{P_r}{P_c} \geq 0.2 \qquad \frac{P_r}{P_c} + \frac{8}{9}\left(\frac{M_{rx}}{M_{cx}} + \frac{M_{ry}}{M_{cy}}\right) \leq 1.0 \tag{6}$$

$$\text{When } \frac{P_r}{P_c} < 0.2 \qquad \frac{P_r}{2P_c} + \left(\frac{M_{rx}}{M_{cx}} + \frac{M_{ry}}{M_{cy}}\right) \leq 1.0 \tag{7}$$

where P_r is the design axial force;
P_c is the axial buckling resistance;
M_{rx}, M_{ry} are the design moments about the major (x) and the minor (y) axes respectively; and
M_{cx}, M_{cy} are the moment resistances about the major (x) and the minor (y) axes respectively.

In the first terms of Eqs. (6) and (7), P_c is related to the in-plane buckling behavior, and it is determined from the studies on columns under axial compression. In this standard, there is only one column curve for the calculation of buckling resistances of all types of steel columns, the applicability of this column curve will be examined later. In the second and third terms, M_{cx} is the lower value obtained according to the limit states of yielding, lateral-torsional buckling and compression flange local buckling. In the calculation of M_{cx} herein, the limit state of lateral-torsional buckling was neglected. M_{cy} is the lower value obtained according to the limit states of yielding and flange local buckling.

Figure 16 depicts the normalized compression and major axis bending relationships of FE models together with design results. Most of the FE results scattered closely to the design results. A few slightly unsafe design results occurred in Sections H1, H2 and H3. The average ratios of FE to design buckling resistances by using curve a and curve b are summarized in Table 9. It is found that all the ratios are larger than 1.00 with standard deviations no greater than 0.05. The minimum value of all the ratios is 0.97. That means the design rules in ANSI/AISC 360-16 could provide accurate predictions to buckling resistances of Q690 steel columns of welded H-sections under combined compression and major axis bending.

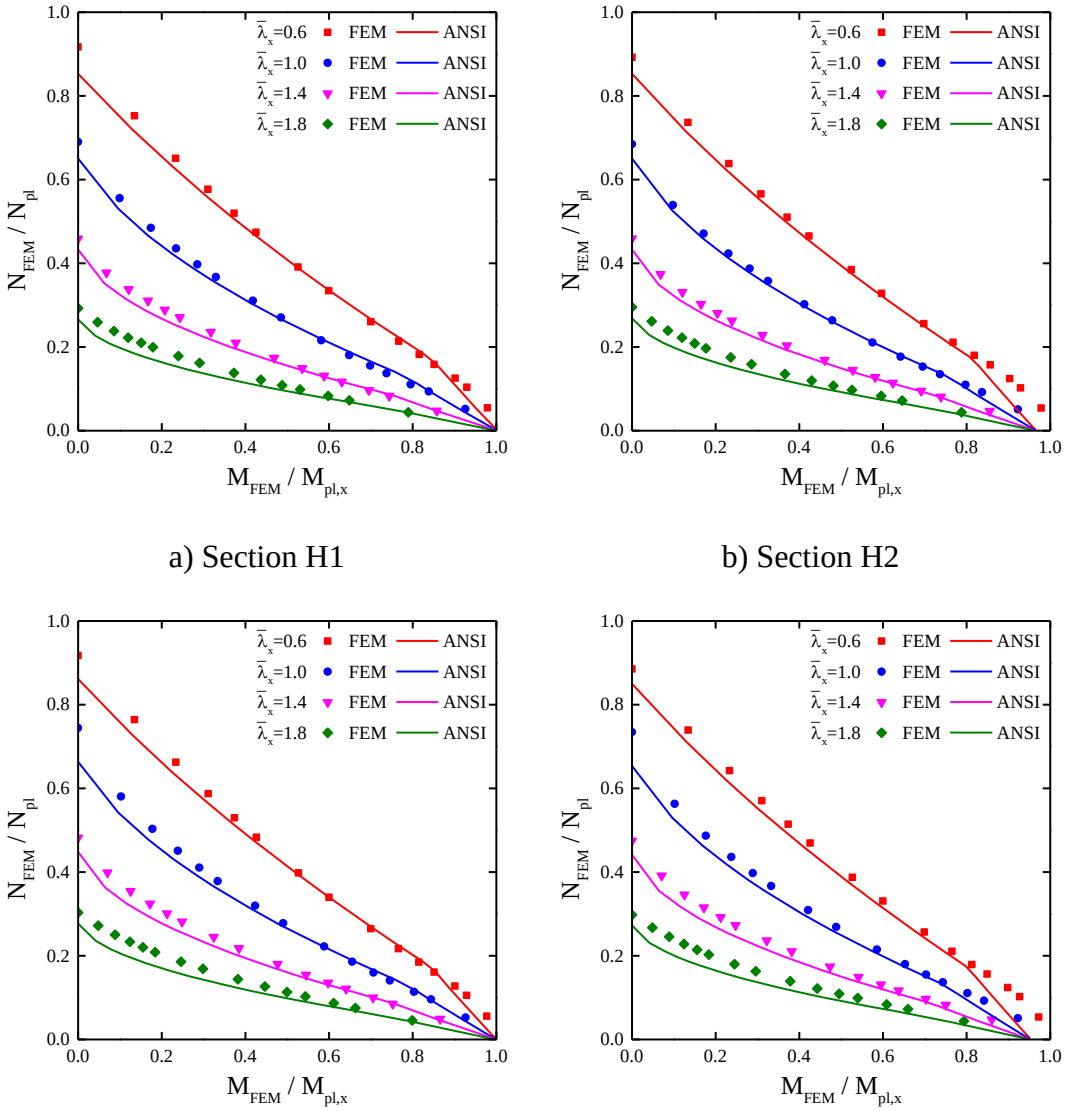

a) Section H1

b) Section H2

c) Section H3

d) Section H4

538 **Figure 16 Normalized compression and major axes bending relationships of FE**
539 **models and design results according to ANSI/AISC 360-16**

540 **Table 9 Ratios of FE to design buckling resistances about major axes according**
541 **to ANSI/AISC 360-16**

H-sections	Average	Standard deviation
H1	1.04	0.05
H2	1.04	0.04
H3	1.05	0.05
H4	1.06	0.04

542

Figure 17 depicts the normalized compression and major axis bending relationships of FE models together with design results. It can be seen that most of the FE results scattered closely to the design results. Overestimations in design values are observed in all the H-sections with various non-dimensional slenderness, especially for Sections H1 and H2 with non-dimensional slenderness of 1.0. The average ratios of FE to design buckling resistances are summarized in Table 10. It is found that except Section H4, the average ratios for the rest Sections are smaller than 1.00. The minimum value of all the ratios is 0.91. The main reason should be that only one column curve is adopted in this code, and this curve is the mean curve of the band for the group with the largest amount of data in Structural Stability Research Council (SSRC) column categories. Thus, overestimation on buckling resistance of eccentrically compressed columns will occur when neglecting the resistance factors. Therefore, the design rules in ANSI/AISC 360-16 should be arguably considered applicable for designing Q690 steel columns of welded H-sections under combined compression and minor axis bending.

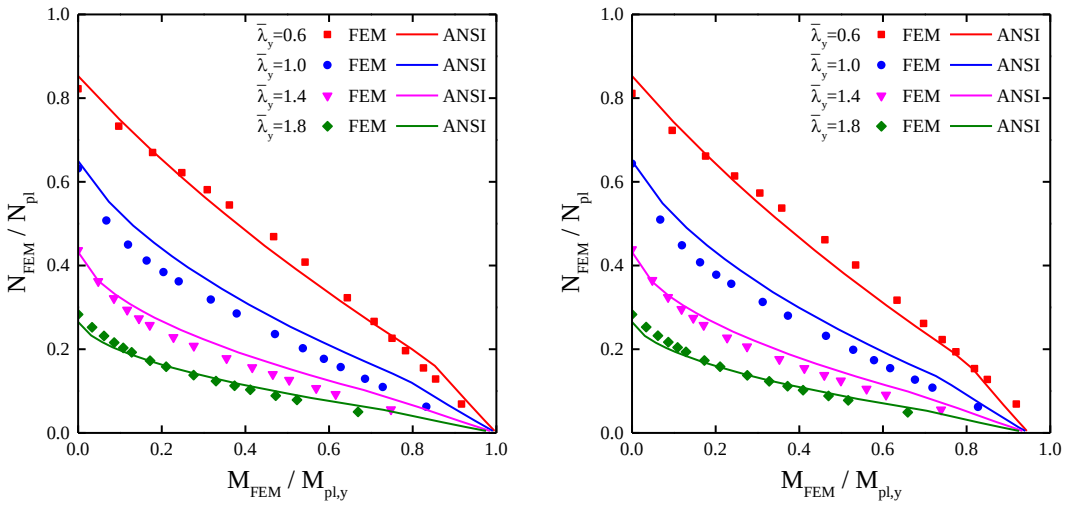

a) Section H1 b) Section H2

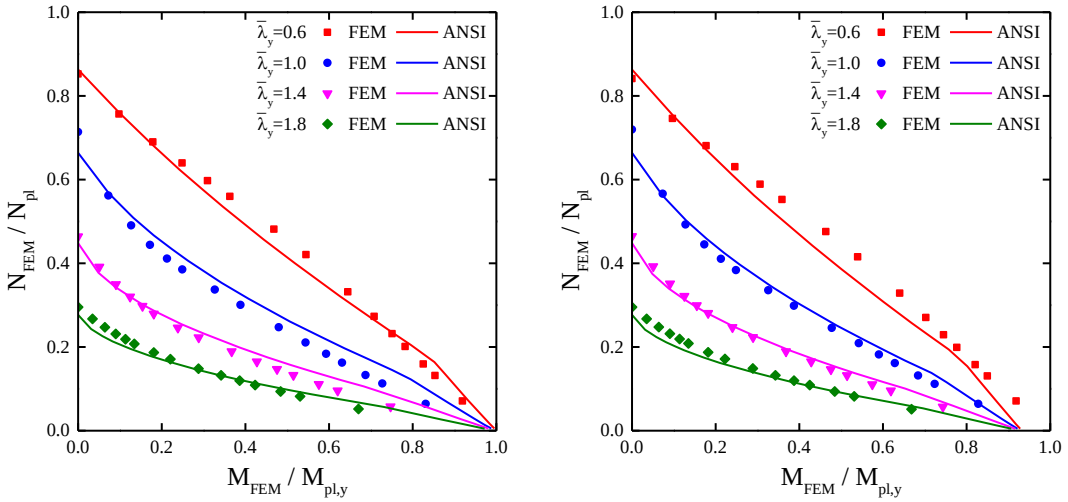

c) Section H3 d) Section H4

Figure 17 Normalized compression and minor axes bending relationships of FE models and design results according to ANSI/AISC 360-16

Table 10 Ratios of FE to design buckling resistances about minor axes according to ANSI/AISC 360-16

H-sections	Average	Standard deviation
H1	0.97	0.05
H2	0.98	0.05
H3	0.99	0.05
H4	1.01	0.04

4.3 GB 50017-2003

According to GB 50017-2003, the buckling resistance for a steel member under combined compression and bending should satisfy Eqs. (8) and (9).

$$\frac{N}{\varphi_x A}+\frac{\beta_{mx}M_x}{\gamma_x W_x\left(1-0.8\frac{N}{N'_{Ex}}\right)}+\eta\frac{\beta_{ty}M_y}{\varphi_{by}W_y}\le f \tag{8}$$

$$\frac{N}{\varphi_y A}+\eta\frac{\beta_{tx}M_x}{\varphi_{bx}W_x}+\frac{\beta_{my}M_y}{\gamma_y W_y\left(1-0.8\frac{N}{N'_{Ey}}\right)}\le f \tag{9}$$

where N is the design value of the compression force;

M_x, M_y are the design moments about the major (x) and the minor (y) axes, respectively;

φ_x, φ_y are the reduction factors for flexural buckling about the major (x) and the minor (y) axes, respectively;

φ_{bx} is the reduction factor for lateral-torsional buckling;

φ_{by} =1.0 ;

N'_{Ex} $= \pi^2 EA / (1.1\lambda_x^2)$;

N'_{Ey} $= \pi^2 EA / (1.1\lambda_y^2)$;

λ_x, λ_y are the slendernesses for flexural buckling about the major (x) and the minor (y) axes, respectively;

A is the cross-sectional area;

W_x, W_y are the elastic moduli about the major (x) and the minor (y) axes, respectively;

β_{mx}, β_{my} are equivalent moment factors for in-plane stability about the major (x) and the minor (y) axes, respectively;

β_{tx}, β_{ty} are equivalent moment factors for out-of-plane stability about the major (x) and the minor (y) axes, respectively;

γ_x, γ_y are plasticity adaptation factors for bending about the major (x) and the minor (y) axes, respectively;

η =1.0 for members susceptible to torsional deformation;
=0.7 for members not susceptible to torsional deformation;

f design yield strength of the steel material; and

E is Young's modulus of the steel material.

In the first terms of Eqs. (8) and (9), the reduction factors, φ_x and φ_y, are related to the in-plane buckling behavior, and they are determined from the studies on columns under axial compression. Curve b is recommended to calculate column buckling resistances of welded H-sections with steel grades no grater than Q420 steel. The assessment of column curve b and a higher column curve, curve a, for designing Q690 steel columns of welded H-sections will be conducted later. In the second term of Eq. (9), the reduction factor φ_{bx} is related to the lateral-torsional buckling behavior and it was taken to be 1.0 in calculations of design buckling resistances.

In this design code, the cross-sectional plastic moduli are evaluated by the product of plasticity adaption factors and cross-sectional elastic moduli. For welded H-sections, the plasticity adaption factors for major (x) and minor (y) axes bending are taken to be 1.05 and 1.20 respectively. That may lead to a partial use of plastic bending resistances of compact and non-compact sections.

Figure 18 depicts the normalized compression and major axis bending relationships of FE models together with design results using curves a and b respectively. It is found that most of the FE results lie closely above the design results by using curve a and only

a few lie closely below. The average ratios of FE to design buckling resistances by using curve a and curve b are summarized in Table 11. It is found that the average ratios using curve a are slightly larger than 1.00 with standard variations no greater than 0.04. The minimum value of all the ratios using curve a is 0.97. Noting that the selection of column curves in this code is based on the "mean value" criteria, slight un-conservatism should be allowed. Therefore, the design rules using curve a could provide accurate predictions to buckling resistances of Q690 steel columns of welded H-sections under combined compression and major axis bending.

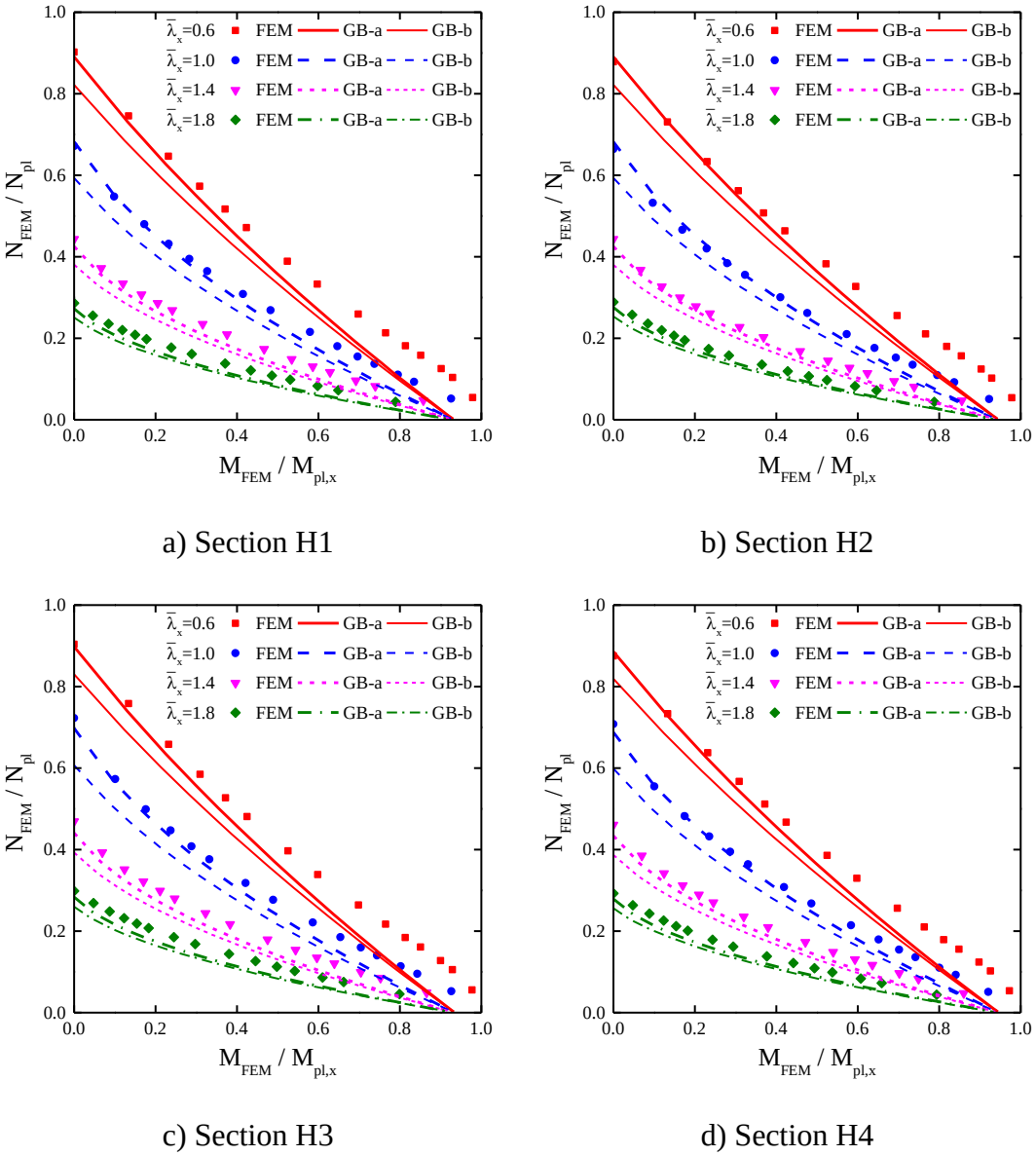

a) Section H1 b) Section H2

c) Section H3 d) Section H4

Figure 18 Normalized compression and major axes bending relationships of FE models and design results according to GB 50017-2003

Table 11 Ratios of FE to design buckling resistances about major axes according to GB 50017-2003

H-sections	Design with curve a		Design with curve b	
	Average	Standard deviation	Average	Standard deviation
H1	1.07	0.04	1.12	0.02
H2	1.05	0.04	1.10	0.02
H3	1.08	0.03	1.13	0.02
H4	1.06	0.03	1.11	0.03

Figure 19 depicts the normalized compression and minor axis bending relationships of FE models together with design results using curves a and b respectively. It can be seen that most of the FE results lie above the design results using curve b and some FE results lie slightly below. The average ratios of FE to design buckling resistances by using curve a and curve b are summarized in Table 12. All the average ratios using curve a are greater than 1.00 but the standard deviations approach 0.10. This is because some FE results are significantly higher than the design results using curve a. All the average ratios using curve b are significantly larger than 1.10 and their standard deviations are relatively reduced. The minimum value of all the ratios using curve b is 0.98. Therefore, the design rules using curve b could make predictions with satisfactory accuracy to buckling resistances of Q690 steel columns of welded H-sections under combined compression and minor axis bending.

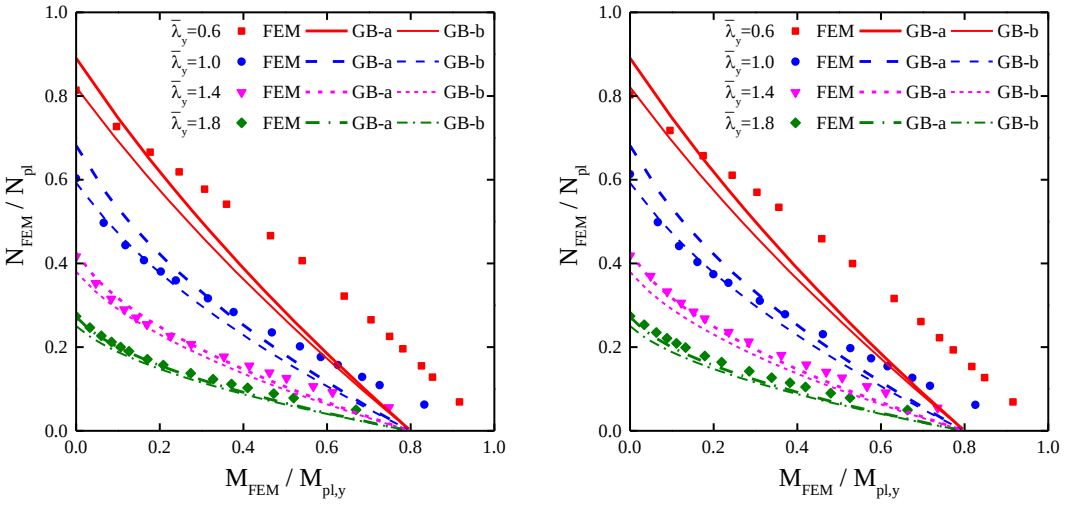

a) Section H1 b) Section H2

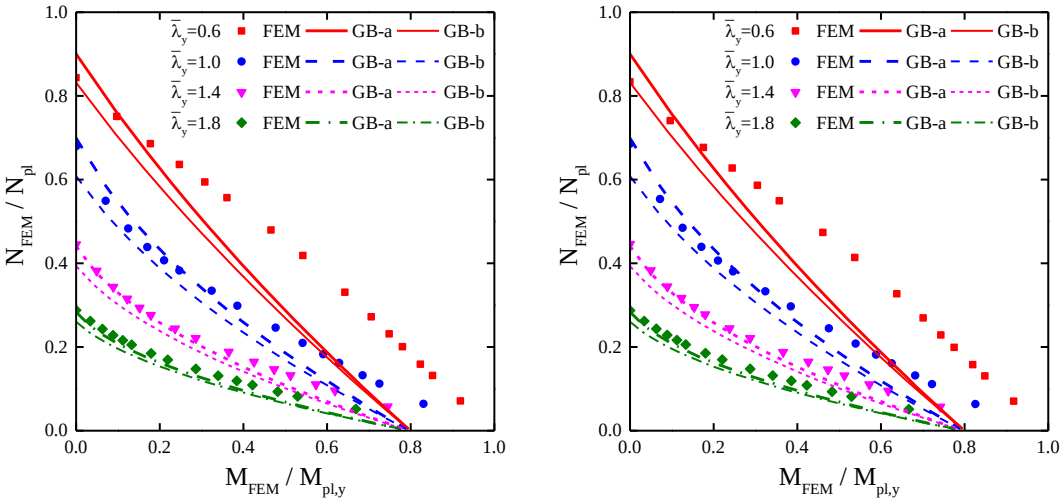

c) Section H3 d) Section H4

Figure 19 Normalized compression and minor axes bending relationships of FE models and design results according to GB 50017-2003

Table 12 Ratios of FE to design buckling resistances about minor axes according to GB 50017-2003

H-sections	Design with curve a		Design with curve b	
	Average	Standard deviation	Average	Standard deviation
H1	1.06	0.10	1.11	0.08
H2	1.07	0.09	1.11	0.07
H3	1.08	0.08	1.13	0.06
H4	1.08	0.08	1.13	0.06

5 Conclusions

This research aims to provide theoretical knowledge on the structural behavior of Q690 steel columns of welded H-sections under combined compression and bending and to make supplementary design proposals based on current design codes. An advanced numerical modeling programme was initially conducted to replicate the experimental results of Q690 steel columns of welded H-sections under combined compression and bending. After validation of the FE models, parametric studies were carried out to investigate the effect of member residual stresses and material tensile to yield strength ratio on buckling resistances of Q690 steel columns of welded H-sections. The assessment of current design rules given in EN 1993-1-1, ANSI/AISC 360-16 and GB 50017-2003 to Q690 steel columns of welded H-sections under combined compression

and bending is performed through the calibration of design buckling resistances against finite element results. The following conclusions have been made:

1) The finite element models incorporating material and geometrical non-linearities can accurately replicate the key test results;

2) The presence of residual stresses can significantly reduce the buckling resistances of Q690 steel columns of welded H-sections under combined compression and bending. Compared with Q235 steel columns of welded H-sections with the same non-dimensional slendernesses and initial loading eccentricity ratios, the effect of residual stresses becomes less on Q690 steel columns of welded H-sections;

3) Strain hardening can barely improve the buckling resistances of Q690 steel columns of welded H-sections and the neglection of strain hardening will not result in a conservative design;

4) In determination of design buckling resistances of Q690 steel columns of welded H-sections under combined compression and major axis bending, the design rules in EN 1993-1-1 using curve a, the design rules in ANSI/AISC 360-16 using the single curve and the design rules in GB 5007-2003 using curve a are proposed;

5) In determination of design buckling resistances of Q690 steel columns of welded H-sections under combined compression and minor axis bending, the design rules in EN 1993-1-1 using curve c, the design rules in ANSI/AISC 360-16 using the single curve and the design rules in GB 5007-2003 using curve b are proposed.

Acknowledgement

The authors are grateful to the financial support provided by the National Natural Science Foundation of China (Granted Project No. 51378378) and the Research Grant Council of the Government of Hong Kong SAR (Project No. PolyU 152194/15E). The project leading to the publication of this paper is also partially funded by the Research Committee (Project Nos. 4-9A6X, RTZX and RTK3) and the Chinese National Engineering Research Centre for Steel Construction (Hong Kong Branch) (Project No. 1-BBY3 & 4) of the Hong Kong Polytechnic University. The research studentships of the first author provided by the Tongji University and the Hong Kong Polytechnic University are also acknowledged.

Reference

[1] T. Y. Ma, Y. F. Hu, X. Liu, G. Q. Li, and K. F. Chung, 'Experimental Investigation into High-strength Q690-steel columns of welded H-sections under Combined Compression and Bending', *J. Constr. Steel Res.*, vol. 138, pp. 449–462, 2017.

[2] K. J. R. Rasmussen and G. J. Hancock, 'Plate slenderness limits for high strength steel sections', *J. Constr. Steel Res.*, vol. 23, pp. 73–96, 1992.

[3] D.-K. Kim, C.-H. Lee, K.-H. Han, J.-H. Kim, S.-E. Lee, and H.-B. Sim, 'Corrigendum to "Strength and residual stress evaluation of stub columns fabricated from 800 MPa high-strength steel"', *J. Constr. Steel Res.*, vol. 113, pp. 286–287, 2015.

[4] G. Shi, W. Zhou, Y. Bai, and C. Lin, 'Local buckling of 460MPa high strength steel welded section stub columns under axial compression', *J. Constr. Steel Res.*, vol. 100, pp. 60–70, 2014.

[5] G. Shi, W. J. Zhou, and C. C. Lin, 'Experimental Investigation on the Local Buckling Behavior of 960 MPa High Strength Steel Welded Section Stub Columns', *Adv. Struct. Eng.*, vol. 18, no. 3, pp. 423–437, 2015.

[6] B. Yuan, 'Local Buckling of High Strength Steel W-Shaped Sections', McMaster University, 1997.

[7] Y. B. Wang, G. Q. Li, S. W. Chen, and F. F. Sun, 'Experimental and numerical study on the behavior of axially compressed high strength steel columns with H-section', *Eng. Struct.*, vol. 43, pp. 149–159, 2012.

[8] Y. B. Wang, G. Q. Li, S. W. Chen, and F. F. Sun, 'Experimental and numerical study on the behavior of axially compressed high strength steel box-columns', *Eng. Struct.*, vol. 58, pp. 79–91, 2014.

[9] H. Y. Ban, G. Shi, Y. J. Shi, and Y. Q. Wang, 'Overall buckling behavior of 460MPa high strength steel columns: Experimental investigation and design method', *J. Constr. Steel Res.*, vol. 74, pp. 140–150, 2012.

710 [10] F. Zhou, L. W. Tong, and Y. Y. Chen, ‘Experimental and numerical
711 investigations of high strength steel welded h-section columns’, *Int. J. Steel*
712 *Struct.*, vol. 13, no. 2, pp. 209–218, Jul. 2013.

713 [11] K. J. R. Rasmussen and G. J. Hancock, ‘Tests of high strength steel columns’, *J.*
714 *Constr. Steel Res.*, vol. 34, no. 1, pp. 27–52, 1995.

715 [12] H. Y. Ban, G. Shi, Y. J. Shi, and M. A. Bradford, ‘Experimental investigation of
716 the overall buckling behaviour of 960MPa high strength steel columns’, *J.*
717 *Constr. Steel Res.*, vol. 88, pp. 256–266, 2013.

718 [13] G. Shi, H. Y. Ban, and F. S. K. Bijlaard, ‘Tests and numerical study of ultra-high
719 strength steel columns with end restraints’, *J. Constr. Steel Res.*, vol. 70, pp.
720 236–247, 2012.

721 [14] D. K. Kim, C. H. Lee, K. H. Han, J. H. Kim, S. E. Lee, and H. B. Sim, ‘Strength
722 and residual stress evaluation of stub columns fabricated from 800MPa high-
723 strength steel’, *J. Constr. Steel Res.*, vol. 102, pp. 111–120, Nov. 2014.

724 [15] American Institute of Steel Construction, *Specification for Structural Steel*
725 *Buildings*. United States: American Institute of Steel Construction, 2010.

726 [16] S.-D. Nie, S.-B. Kang, L. Shen, and B. Yang, ‘Experimental and numerical study
727 on global buckling of Q460GJ steel box columns under eccentric compression’,
728 *Eng. Struct.*, vol. 142, pp. 211–222, 2017.

729 [17] T. Usami and Y. Fukumoto, ‘Local and Overall Buckling of Welded Box
730 Columns’, *J. Struct. Div.*, vol. 108, no. 3, pp. 525–542, 1982.

731 [18] T. Usami and Y. Fukumoto, ‘Welded box compression members’, *J. Struct. Eng.*,
732 vol. 110, no. 10, pp. 2457–2470, 1984.

733 [19] H. X. Shen, ‘Behavior of high-strength steel welded rectangular section beam-
734 columns with slender webs’, *Thin-Walled Struct.*, vol. 88, pp. 16–27, 2015.

735 [20] Ministry of Construction of the People’s Republic of China, *GB 50017-2003.*
736 *Code for Design of Steel Structures*. Beijing: China Architecture and Building
737 Press, 2003.

738 [21] European Committee for Standardization (CEN), *Eurocode 3 - Design of steel*
739 *structures - Part 1-1: General rules and rules for buildings*. Belgium: Brussels,
740 2005.

[22] European Committee for Standardization (CEN), *Eurocode 3 - Design of steel structures - Part 1-12 : Additional rules for the extension of EN 1993 up to steel grades S 700*. Belgium: Brussels, 2007.

[23] American Institute of Steel Construction, *Specification for Structural Steel Buildings*. United States: American Institute of Steel Construction, 2016.

[24] L. Gao, H. C. Sun, F. N. Jin, and H. L. Fan, 'Load-carrying capacity of high-strength steel box-sections I: Stub columns', *J. Constr. Steel Res.*, vol. 65, no. 4, pp. 918–924, Apr. 2009.

[25] S. M. Chou, G. B. Chai, and L. Ling, 'Finite element technique for design of stub columns', *Thin-Walled Struct.*, vol. 37, no. 2, pp. 97–112, 2000.

[26] O. Zhao, B. Rossi, L. Gardner, and B. Young, 'Behaviour of structural stainless steel cross-sections under combined loading – Part II: Numerical modelling and design approach', *Eng. Struct.*, vol. 89, pp. 247–259, 2015.

[27] X. Liu and K. F. Chung, 'Eerimental investigation into residual stresses of welded H-sections made of Q690 steel materials', in *The 14th East Asia-Pacific Conference on Structural Engineering and Construction*, 2016, pp. 559–565.

[28] Ministry of Construction of the People's Republic of China, *GB/T 700. Carbon structural steels*. 2006.

[29] European Committee for Standardization (CEN), *Hot rolled products of structural steels - Part 2: Technical delivery conditions for non-alloy structural steels*. Belgium: Brussels, 2004.

[30] H. Y. Ban, G. Shi, Y. J. Shi, and Y. Q. Wang, 'Research advances on mechanical properties of high strength structural steels', *Build. Struct.*, vol. 43, no. 2, pp. 88–94, 2013.

[31] T. V. Galambos, *Guide to stability design criteria for metal structures*, 5th ed. John Wiley & Sons, 1998.